

# Optimal Data Detection in Large MIMO

Charles Jeon, Ramina Ghods, Arian Maleki, and Christoph Studer

## Abstract

Large multiple-input multiple-output (MIMO) appears in massive multi-user MIMO and randomly-spread code-division multiple access (CDMA)-based wireless systems. In order to cope with the excessively high complexity of optimal data detection in such systems, a variety of efficient yet sub-optimal algorithms have been proposed in the past. In this paper, we propose a data detection algorithm that is computationally efficient and optimal in a sense that it is able to achieve the same error-rate performance as the individually optimal (IO) data detector under certain assumptions on the MIMO system matrix and constellation alphabet. Our algorithm, which we refer to as LAMA (short for LArge MIMO AMP), builds on complex-valued Bayesian approximate message passing (AMP), which enables an exact analytical characterization of the performance and complexity in the large-system limit via the state-evolution framework. We derive optimality conditions for LAMA and investigate performance/complexity trade-offs. As a byproduct of our analysis, we recover classical results of IO data detection for randomly-spread CDMA. We furthermore provide practical ways for LAMA to approach the theoretical performance limits in realistic, finite-dimensional systems at low computational complexity.

## Index Terms

Approximate message passing (AMP), individually optimal (IO) data detection, massive multi-user MIMO, state evolution, randomly-spread code-division multiple access (CDMA).

## I. INTRODUCTION

We consider the problem of recovering the  $M_T$ -dimensional data vector  $\mathbf{s}_0 \in \mathcal{O}^{M_T}$  from the noisy input-output relation  $\mathbf{y} = \mathbf{H}\mathbf{s}_0 + \mathbf{n}$ , by solving the individually-optimal (IO) data detection

This paper was presented in part at the 2015 International Symposium on Information Theory (ISIT) [1].

C. Jeon, R. Ghods, and C. Studer are with the School of Electrical and Computer Engineering, Cornell University, Ithaca, NY; e-mail: jeon@cs.cornell.edu, rghods@cs.cornell.edu, studer@cornell.edu; web: vip.ece.cornell.edu

A. Maleki is with Department of Statistics at Columbia University, New York City, NY; e-mail: arian@stat.columbia.edu.

MATLAB code to reproduce our numerical simulations will be made available upon (possible) acceptance of paper.

problem [2], [3]

$$(IO) \quad s_\ell^{\text{IO}} = \arg \max_{\tilde{s}_\ell \in \mathcal{O}} p(\tilde{s}_\ell | \mathbf{y}, \mathbf{H}), \quad \ell = 1, 2, \dots, M_T,$$

where  $p(\tilde{s}_\ell | \mathbf{y}, \mathbf{H})$  is the probability density function conditioned on observing the receive vector  $\mathbf{y} \in \mathbb{C}^{M_R}$  and assuming Gaussian noise for the noise vector  $\mathbf{n} \in \mathbb{C}^{M_R}$ . The scalar  $s_\ell^{\text{IO}}$  corresponds to the  $\ell$ th IO estimate,  $\mathcal{O}$  is a finite constellation set (e.g., PAM, PSK, or QAM),  $M_T$  and  $M_R$  denote the number of transmitters and receivers, respectively, and  $\mathbf{H} \in \mathbb{C}^{M_R \times M_T}$  represents the (known) multiple-input multiple-output (MIMO) channel matrix.

We develop a computationally efficient algorithm, referred to as LAMA (short for large MIMO approximate message passing), which is able to achieve the error-rate performance of the IO data-detector under certain assumptions on the MIMO channel matrix and the constellation alphabet. We show that in the large system limit, i.e., for  $\beta = M_T/M_R$  and  $M_T \rightarrow \infty$ , and for i.i.d. Rayleigh fading MIMO channels, LAMA decouples the noisy MIMO system into a set of independent additive white Gaussian noise (AWGN) channels with equal signal-to-noise ratio (SNR); see Fig. 1 for an illustration of this decoupling property. LAMA is iterative in nature and enables one to compute the noise variance  $\sigma_t^2$  of each decoupled AWGN channel in each iteration  $t$ . This property allows for a precise analysis of the algorithm's performance (in terms of achievable rates and error rate) and complexity (in terms of the number of LAMA iterations).

Figure 2(a) demonstrates that LAMA (i) is able to achieve the error-rate performance of the individually optimal detector for a square MIMO system (i.e.,  $M_R = M_T$ ) in the large-system limit, and (ii) closely approaches the error-rate performance of the IO data detector in finite-dimensional systems. Furthermore, we can accurately characterize the performance/complexity trade-offs without the need for expensive system simulations; see Fig. 2(b) for an illustration.

### A. Application Examples

The considered MIMO system model covers a variety of applications, including the following examples.

1) *Massive Multi-User (MU) MIMO*: Massive MU-MIMO (also known as large-scale or full-dimensional MIMO) will be a key technology to meet the demands for higher spectral efficiency and quality-of-service-in fifth-generation (5G) wireless systems [4]–[6]. Massive MU-MIMO relies on hundreds of antennas at the base-station (BS) that serve tens of users simultaneously and in the same frequency band. This technology promises significant gains in terms of spectral efficiency

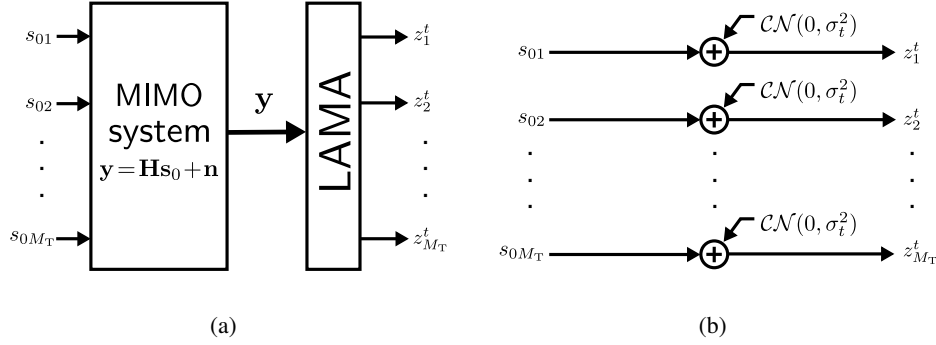


Fig. 1. Decoupling property of LAMA. (a) Large MIMO system. (b) LAMA decouples the system into parallel and independent AWGN channels with equal noise variance in the large-system limit ( $\beta = M_T/M_R$  and  $M_T \rightarrow \infty$ ). The state-evolution (SE) framework provides exact expressions for the AWGN noise variance  $\sigma_t^2$  at iteration  $t$ , which enables a precise analysis of LAMA's performance (in terms of achievable rates and error rate) and complexity (in terms of the number of algorithm iterations).

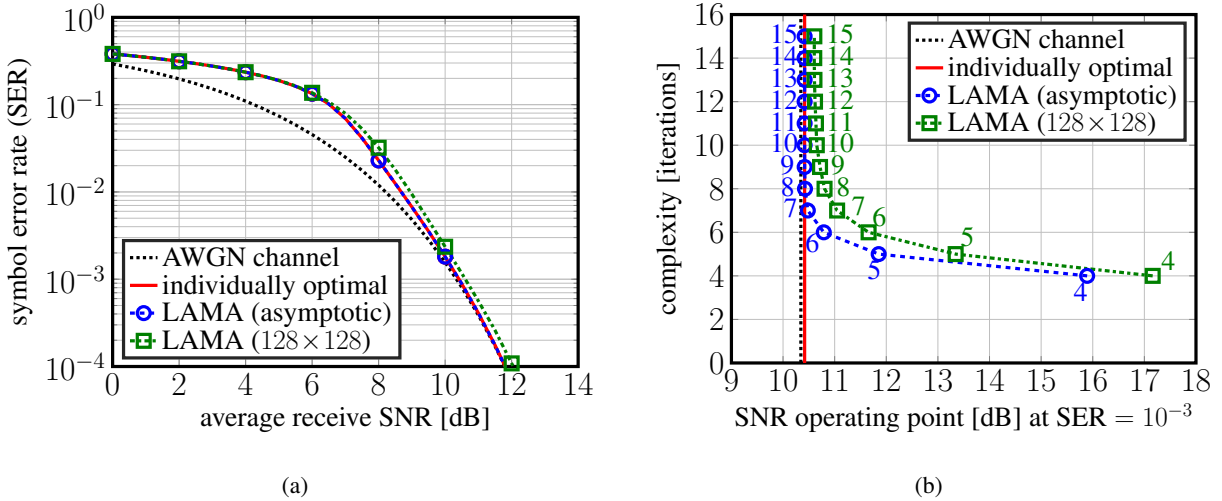


Fig. 2. Capabilities of LAMA in large MIMO with a square i.i.d. Gaussian system matrix and QPSK modulation. (a) Symbol error-rate (SER) in the large-system limit ( $\beta = M_T/M_R = 1$  and  $M_T \rightarrow \infty$ ) compared to the optimal SER and the SER of an AWGN channel. LAMA achieves the same error-rate performance as the IO data detector and approaches AWGN performance for sufficiently large SNR values; we also see that LAMA closely approaches the theoretical performance limits for finite dimensions (i.e., for a  $128 \times 128$  MIMO system). (b) Performance/complexity trade-off in the large-system limit (analytical) and for finite dimensions (simulated); a small number of LAMA iterations is sufficient to approach the theoretical performance limits.

as well as lower operational power consumption compared to that of existing, small-scale MIMO systems [5]. In addition, in the large BS-antenna limit, i.e., where  $M_R \rightarrow \infty$  and the total number  $M_T$  of user antennas remains constant, low-complexity data detection and precoding methods (such as the matched filter) turn out to be optimal [7]. However, as demonstrated in [8]–[10], practical (finite-dimensional) antenna configurations require more sophisticated data detection

algorithms, which entail high computational complexity. The proposed LAMA algorithm enables high-performance and low-complexity data detection in practical massive MU-MIMO systems with higher-order modulation schemes, and allows for an accurate prediction of the fundamental performance/complexity trade-offs.

2) *Code-Division Multiple Access (CDMA)*: CDMA is a classical transmission technology, in which multiple users simultaneously access a common resource (such as time or frequency) by modulating their individual information signals using spreading sequences [11]–[15]. A significant portion of the CDMA literature studied the limits (such as the achievable rates for a given modulation scheme) of randomly spread CDMA. In the considered system model, the spreading matrix corresponds to  $\mathbf{H}$  with i.i.d. zero-mean Gaussian entries,  $M_T$  denotes the number of users, and the spreading sequences are of length  $M_R$ . For common constellations (such as PAM, PSK, or QAM), we provide conditions that depend on the *system ratio*  $\beta = M_T/M_R$  (also known as the loading factor) in the large-system limit for which LAMA achieves the same error-rate performance of the IO data detector [3]. Our analysis recovers classical results from the CDMA literature [3], [16], [17] while providing practical means for closely approaching these limits in finite-dimensional systems at low computational complexity.

3) *Finding Discrete Solutions to Systems of Linear Equations*: The considered system model also enables one to study the recovery of integer solutions to the (noisy) system of linear equations  $\mathbf{y} = \mathbf{H}\mathbf{s} + \mathbf{n}$ . For noiseless observations, i.e.,  $\mathbf{y} = \mathbf{H}\mathbf{s}$ , and for the case of  $\mathcal{O}$  being (a subset of) the integers, LAMA is able to perfectly recover  $\mathbf{s} \in \mathcal{O}^{M_T}$  provided that the entries of the system matrix  $\mathbf{H}$  are i.i.d. zero-mean Gaussian distributed and the system ratio  $\beta = M_T/M_R$  does not exceed a certain *exact recovery threshold (ERT)*. This result is relevant for solving systems of linear Diophantine equations, which finds, for example, use in number theory, cryptography, or closest vector problems in lattices; see [18]–[21] and the references therein.

## B. Relevant Prior Results

Early results on optimal data detection in large MIMO systems reach back to [22] where Verdú and Shamai analyzed the spectral efficiency of multi-user detectors in randomly-spread CDMA systems. The authors provided a precise characterization of the achievable rates with optimal data detection and demonstrated that the system's randomness (due to the random spreading sequences) disappears in the large-system limit. Tanaka [16] derived analytical expressions for the error-rate performance and the multi-user efficiency (equivalent to the noise variance in a single

AWGN channel) for the IO data detector using the replica method [23]; Tanaka’s results were obtained for BPSK constellations using the replica method in [16] and later proven rigorously in [24]. Guo and Verdú provided an extension of these results to arbitrary discrete inputs [3]. Moreover, it was shown that for a certain family of multi-user detectors, referred as posterior mean estimators (PMEs), the communication system decouples into a set of parallel and independent AWGN channels with equal SNR [3], [16], [25], [26]. All of these results study the fundamental performance of IO detection in the large-system limit, i.e., for  $\beta = M_T/M_R$  with  $M_T \rightarrow \infty$ . Corresponding practical algorithms have been proposed for BPSK in real-valued systems [17], [27]—in contrast, LAMA is a practical algorithm for general constellations and complex-valued systems, and enables a corresponding theoretical performance analysis.

LAMA builds upon approximate message passing (AMP) [28]–[30], which was initially proposed for sparse signal recovery and compressive sensing [31]–[33]. In the large-system limit, the estimates obtained by AMP correspond to the true signal perturbed by i.i.d. Gaussian noise [34]. In addition, the variance of the Gaussian random variables in each AMP iteration can be tracked exactly via the state evolution (SE) framework [28], [29]; this feature enables an exact performance analysis. AMP has been generalized to i.i.d. signal priors using the Bayesian AMP framework [30], [35], [36] and to sparse recovery in complex-valued systems [37]. More recently, AMP and the SE framework have been extended to more general observation models in [38]–[40]. Within the last few years, AMP has been successfully deployed in a variety of applications [41]–[44], including signal restoration [45], [46], imaging [47], phase retrieval [48], and de-noising [33], [49]. AMP-related algorithms have also been used for data detection in many different communication systems [45], [50]–[53]. While these results showcase the potential of AMP for data detection in wireless systems, they lack of a rigorous performance analysis. In this paper, we focus on a theoretical performance analysis of AMP for data detection and provide conditions for which it achieves IO performance.

### *C. Contributions*

In this paper, we build upon complex-valued AMP [37] and (real-valued) Bayesian AMP [30] in order to develop the complex Bayesian AMP (cB-AMP) algorithm and its complex state evolution (cSE) framework. Our derivations incorporate the possibility of having a mismatch between the actual and a postulated noise variance. We then specialize cB-AMP to data detection in large MIMO, resulting in the LAMA algorithm. Our key contributions are as follows.

- We study LAMA in the massive MU-MIMO limit, i.e., when  $\beta \rightarrow 0$ , and show that for such a scenario, simple low-complexity algorithms achieve IO performance.
- We demonstrate that the SE recursions of LAMA are identical to the fixed-point equations that predict the optimal multiuser efficiency developed in [3], [16], [25].
- We develop conditions for which LAMA achieves the same error-rate performance as the IO data detector.
- We derive exact recovery thresholds (ERTs), for which LAMA perfectly recovers signals from PAM, PSK, and QAM alphabets in noiseless systems.
- We investigate the achievable rates and error-rate performance of LAMA for PAM, PSK, and QAM constellations, and analyze the impact of the system ratio  $\beta$ .
- We characterize the performance/complexity trade-off of LAMA and show that only a few algorithm iterations are sufficient to achieve near-IO performance.
- We discuss the efficacy and limits of the proposed LAMA algorithms in practical (finite-dimensional) large-MIMO systems and provide corresponding numerical results.

#### D. Notation

Lowercase and uppercase boldface letters represent column vectors and matrices, respectively. For a matrix  $\mathbf{H}$ , we define its transpose and Hermitian to be  $\mathbf{H}^T$  and  $\mathbf{H}^H$ , respectively. The  $\ell$ th column and the  $k$ th row vector of the matrix  $\mathbf{H}$  are denoted by  $\mathbf{h}_\ell^c$  and  $\mathbf{h}_k^r$ , respectively, the entry on the  $k$ th row and  $\ell$ th column is  $H_{k,\ell}$ , and the  $k$ th entry of a vector  $\mathbf{x}$  is  $x_k$ . For a  $N$ -dimensional vector  $\mathbf{x}$ , we define its complex conjugate by  $\mathbf{x}^*$  and its  $k$ th entry by  $x_k$ . The  $M \times M$  identity matrix is denoted by  $\mathbf{I}_M$  and the  $M \times N$  all-zeros matrix by  $\mathbf{0}_{M \times N}$ . The real and imaginary parts of scalars, vectors, and matrices are denoted by  $\text{Re}\{\cdot\}$  and  $\text{Im}\{\cdot\}$ , respectively. We use  $\langle \cdot \rangle$  to represent the averaging operator  $\langle \mathbf{x} \rangle = \frac{1}{N} \sum_{k=1}^N x_k$ . Multivariate real-valued and complex-valued Gaussian probability density (pdf) functions are denoted by  $\mathcal{N}(\mathbf{m}, \mathbf{K})$  and  $\mathcal{CN}(\mathbf{m}, \mathbf{K})$ , respectively, where  $\mathbf{m}$  is the mean vector and  $\mathbf{K}$  the covariance matrix;  $\mathbb{E}_X[\cdot]$  denotes expectation and  $\mathbb{V}\text{ar}_X[\cdot]$  denotes variance with respect to the pdf of the random variable  $X$ .

#### E. Paper Outline

The rest of the paper is organized as follows. Section II introduces the complex Bayesian AMP (cB-AMP) algorithm and the complex state evolution (cSE) framework. Section III derives the LAMA algorithm. Section IV provides optimality conditions. Section V presents corresponding

numerical results and discusses practical considerations. Section VI summarizes prior art relevant to LAMA and Section VII concludes the paper. All proofs are relegated to the appendices.

## II. CB-AMP: COMPLEX BAYESIAN AMP

We start by developing the complex Bayesian AMP (cB-AMP) framework which builds the foundation of the LAMA algorithm developed in Section III. We specify our model assumptions, derive cB-AMP, and detail the complex-valued state-evolution (cSE) framework.

### A. System Model and Assumptions

We estimate the complex-valued data vector  $\mathbf{s}_0 \in \mathbb{C}^{M_T}$  with known i.i.d. prior distribution  $p(\mathbf{s}_0) = \prod_{\ell=1}^{M_T} p(s_{0\ell})$  from the following MIMO input-output relation:

$$\mathbf{y} = \mathbf{H}\mathbf{s}_0 + \mathbf{n}. \quad (1)$$

The number of transmitters and receivers are denoted by  $M_T$  and  $M_R$ , respectively, and we do not impose any assumption on the so-called *system ratio* (also known as the loading factor in CDMA literature [54]), which we define as  $\beta = M_T/M_R$ . We will often use the following definition:

**Definition 1.** *For a MIMO system with  $M_T$  and  $M_R$  transmitters and receivers respectively, we define the large-system limit by fixing the system ratio  $\beta = M_T/M_R$  and letting  $M_T \rightarrow \infty$ .*

In what follows, we will consider underdetermined ( $\beta \leq 1$ ) as well as overdetermined ( $\beta > 1$ ) systems. The receive vector in (1) is given by  $\mathbf{y} \in \mathbb{C}^{M_R}$  and the entries of the noise vector  $\mathbf{n} \in \mathbb{C}^{M_R}$  are assumed to be i.i.d. circularly-symmetric complex Gaussian with variance  $N_0$  per complex entry. The MIMO system matrix  $\mathbf{H} \in \mathbb{C}^{M_R \times M_T}$  is assumed to be perfectly known to the receiver. We will frequently use of the following assumptions on the MIMO system matrix  $\mathbf{H}$  [34]:

- (A1) The entries of  $\mathbf{H}$  are normalized so that the columns are zero mean and have unit  $\ell_2$ -norm; the real and imaginary parts are independent with identical variance. Furthermore, all entries have similar magnitude  $O(1/\sqrt{M_R})$  and are pairwise independent.
- (A2) The entries  $H_{k,\ell} \sim \mathcal{CN}(0, 1/M_R)$  are i.i.d. circularly-symmetric complex Gaussian.

We note that (A2) implies (A1) in the large-system limit; see [34] for the details. Throughout the paper, we define the average receive signal-to-noise-ratio *SNR* as:

$$SNR = \frac{\mathbb{E}[\|\mathbf{H}\mathbf{s}_0\|_2^2]}{\mathbb{E}[\|\mathbf{n}\|_2^2]} = \beta \frac{E_s}{N_0}, \quad (2)$$

where  $E_s = \mathbb{E}[|s_{0\ell}|^2]$  for all  $\ell = 1, \dots, M_T$ . We also consider the case in which the receiver assumes the following (possibly) mismatched input-output relation:

$$\mathbf{y} = \mathbf{H}\mathbf{s}_0 + \mathbf{n}^{\text{post}}. \quad (3)$$

Here,  $\mathbf{n}^{\text{post}} \sim \mathcal{CN}(0_{M_R \times 1}, N_0^{\text{post}} \mathbf{I}_{M_R})$  models noise with postulated noise variance  $N_0^{\text{post}}$  (not necessarily equal to  $N_0$ ). The model in (3) allows us to analyze a mismatch between the true noise variance  $N_0$  and the postulated noise variance  $N_0^{\text{post}}$  assumed by the detector. The case  $N_0 = N_0^{\text{post}}$  corresponds to an ideal system with perfect knowledge of the noise variance.

### B. Complex Bayesian AMP (cB-AMP)

To arrive at an efficient algorithm that achieves the same error-rate performance as the IO data detector, we start with the Bayesian AMP (B-AMP) algorithm proposed in [30], [35], [36] to obtain a marginalized distribution  $p(\tilde{s}_\ell | \mathbf{y}, \mathbf{H})$  for each stream  $\ell$  (also called layer). With the marginalized distribution, B-AMP enables the estimation of a vector  $\mathbf{s}_0$  from a real-valued version of the system model (1). While B-AMP can—in certain cases—be applied to complex-valued systems using the well-known real-valued decomposition<sup>1</sup>, the effective, real-valued system matrix  $\bar{\mathbf{H}} \in \mathbb{R}^{2M_R \times 2M_T}$  (i) violates the independence assumptions on the entries of  $\mathbf{H}$  of (A1), and (ii) prevents the use of non-separable symbol alphabets, such as phase-shift keying (PSK) constellations. To overcome both of these drawbacks, we develop a complex-valued version of B-AMP, which we refer to as cB-AMP. We start with Bayes' rule and factorize

$$p(\mathbf{y} | \mathbf{s}, \mathbf{H}) p(\mathbf{s}) = \prod_{k=1}^{M_R} p(y_k | \mathbf{s}, \mathbf{h}_k^r) \prod_{\ell=1}^{M_T} p(s_\ell), \quad (4)$$

where we assume (i) complex Gaussian noise with postulated noise variance  $N_0^{\text{post}}$  given by

$$p(y_k | \mathbf{s}, \mathbf{h}_k^r) = \frac{1}{Z} \exp\left(-\frac{1}{N_0^{\text{post}}} |y_k - \mathbf{h}_k^r \mathbf{s}|^2\right),$$

with the constant  $Z$  so that  $\int_{\mathbb{C}} p(y_k | \mathbf{s}, \mathbf{h}_k^r) dy_k = 1$ , and (ii) that the transmitted symbols are i.i.d.

To arrive at an efficient inference method, we deploy the sum-product message-passing algorithm [55]. However, as noted in [28], a corresponding full-fledged message passing scheme

<sup>1</sup>The complex-valued model (1) can be rewritten as the following real-valued model:

$$\begin{bmatrix} \text{Re}\{\mathbf{y}\} \\ \text{Im}\{\mathbf{y}\} \end{bmatrix} = \begin{bmatrix} \text{Re}\{\mathbf{H}\} & -\text{Im}\{\mathbf{H}\} \\ \text{Im}\{\mathbf{H}\} & \text{Re}\{\mathbf{H}\} \end{bmatrix} \begin{bmatrix} \text{Re}\{\mathbf{s}\} \\ \text{Im}\{\mathbf{s}\} \end{bmatrix} + \begin{bmatrix} \text{Re}\{\mathbf{n}\} \\ \text{Im}\{\mathbf{n}\} \end{bmatrix}.$$



is impractical. Hence, as in [30], [34], we simplify the algorithm by assuming a Gaussian distribution for the marginal densities of the messages  $p(\hat{s}_\ell | s_\ell, \tau) \sim \mathcal{CN}(s_\ell, \tau)$  so that [34]

$$\begin{aligned} f(s_\ell | \hat{s}_\ell, \tau) &= \frac{p(\hat{s}_\ell | s_\ell, \tau)p(s_\ell)}{p(\hat{s}_\ell, \tau)} \\ &= \frac{1}{Z'} \exp\left(-\frac{1}{\tau}|s_\ell - \hat{s}_\ell|^2\right)p(s_\ell), \end{aligned} \quad (5)$$

with the normalization constant  $Z'$ . We denote the conditional mean  $F(\hat{s}_\ell, \tau)$  and variance  $G(\hat{s}_\ell, \tau)$  of a random variable  $S$  distributed according to (5) as the message mean and message variance; both quantities are defined as follows:

$$F(\hat{s}_\ell, \tau) = \mathbb{E}_S[S | \hat{s}_\ell, \tau] \quad (6)$$

$$G(\hat{s}_\ell, \tau) = \text{Var}_S[S | \hat{s}_\ell, \tau]. \quad (7)$$

With the methods developed in [30], [37], we can simplify the sum-product message-passing computations for (4) which stems from the Gaussian assumption for the marginal densities of the messages. We refer to the resulting algorithm as complex Bayesian AMP (cB-AMP), which is summarized below (and derived in detail in Appendix B):

**Algorithm 1.** *Suppose that  $\mathbf{H}$  satisfies (A1) and [30, Lem. 5.56] holds. Then, the complex Bayesian AMP (cB-AMP) algorithm performs the following steps for each iteration  $t = 1, 2, \dots$ :*

$$\begin{aligned} \hat{\mathbf{s}}^{t+1} &= F(\hat{\mathbf{s}}^t + \mathbf{H}^H \mathbf{r}^t, N_0^{\text{post}}(1 + \tau^t)) \\ \mathbf{r}^{t+1} &= \mathbf{y} - \mathbf{H}\hat{\mathbf{s}}^{t+1} \\ &\quad + \frac{\beta \mathbf{r}^t}{2} \langle (\partial_1 F^R + \partial_2 F^I)(\hat{\mathbf{s}}^t + \mathbf{H}^H \mathbf{r}^t, N_0^{\text{post}}(1 + \tau^t)) \rangle \\ &\quad - i \frac{\beta \mathbf{r}^t}{2} \langle (\partial_2 F^R - \partial_1 F^I)(\hat{\mathbf{s}}^t + \mathbf{H}^H \mathbf{r}^t, N_0^{\text{post}}(1 + \tau^t)) \rangle \\ \tau^{t+1} &= \frac{\beta}{N_0^{\text{post}}} \langle G(\hat{\mathbf{s}}^t + \mathbf{H}^H \mathbf{r}^t, N_0^{\text{post}}(1 + \tau^t)) \rangle, \end{aligned} \quad (8)$$

where the functions  $\partial_{\{1,2\}} F^{\{R,I\}}(x + iy, \tau)$  are defined as

$$\begin{aligned} \partial_1 F^R &\triangleq \frac{\partial \text{Re}\{F(x + iy, \tau)\}}{\partial x}, & \partial_2 F^R &\triangleq \frac{\partial \text{Re}\{F(x + iy, \tau)\}}{\partial y}, \\ \partial_1 F^I &\triangleq \frac{\partial \text{Im}\{F(x + iy, \tau)\}}{\partial x}, & \partial_2 F^I &\triangleq \frac{\partial \text{Im}\{F(x + iy, \tau)\}}{\partial y}, \end{aligned}$$

and  $\partial_{\{1,2\}} F^{\{R,I\}}$ ,  $F$ , as well as  $G$  operate element-wise on vectors.

We note that  $\hat{\mathbf{s}}^{t+1}$  in Algorithm 1 corresponds to the (nonlinear) minimum mean-squared error (MMSE) estimate defined in (6). For a real-valued system with  $N_0 = N_0^{\text{post}}$ , cB-AMP reduces to the real-valued Bayesian AMP (B-AMP) proposed in [30]; Appendix C establishes this fact.

**Lemma 1.** *Let  $N_0^{\text{post}} = N_0$  and assume  $\mathbf{H}$  satisfies (A1). If  $\mathbf{H}$ ,  $\mathbf{s}$ , and  $\mathbf{n}$  are real-valued, then cB-AMP reduces to B-AMP in [30].*

### C. cSE: Complex State Evolution (with Mismatch)

Two unique features of AMP-based algorithms are (i) the output decouples the system into parallel independent channels with additive Gaussian noise (see Fig. 1 for an illustration), and (ii) the noise variance of the decoupled AWGN channel can be predicted analytically via fixed-point equations in the large-system limit, which is known as *state evolution* (SE) [34]. The SE framework has been investigated in detail in [30] for B-AMP and in [37] for CAMP, which is a special case of cB-AMP proposed here<sup>2</sup>. Before we delve into the complex SE (cSE) framework for analysis on the noise variance of the decoupled AWGN channels, we first define the mean-squared error (MSE) of cB-AMP's MMSE output.

**Definition 2.** *Suppose that  $\mathbf{y} = \mathbf{H}\mathbf{s}_0 + \mathbf{n}$ , where the signal  $\mathbf{s}_0$  is distributed according to  $\mathbf{s}_0 \sim p(\mathbf{s}_0)$ ,  $\mathbf{n} \sim \mathcal{CN}(0_{M_R \times 1}, N_0 \mathbf{I}_{M_R})$ , and the postulated noise variance is  $N_0^{\text{post}}$ . Let  $\hat{\mathbf{s}}^{t+1}$  be the MMSE output of cB-AMP after  $t$  iterations. We define the MSE of the MMSE output of cB-AMP after  $t$  iterations as follows:*

$$\begin{aligned} \text{MSE}_t &= \lim_{M_T \rightarrow \infty} \frac{1}{M_T} \|\hat{\mathbf{s}}^{t+1} - \mathbf{s}_0\|_2^2 \\ &= \lim_{M_T \rightarrow \infty} \frac{1}{M_T} \sum_{\ell=1}^{M_T} |\mathbb{F}(\hat{s}_\ell^t + (\mathbf{h}_\ell^c)^H \mathbf{r}^t, N_0^{\text{post}}(1 + \tau^t)) - s_{0\ell}|^2. \end{aligned} \quad (9)$$

We now define effective noise variance  $\sigma_t^2$ , which represents the noise variance of the decoupled AWGN channel after  $t$  iterations in the large-system limit (see Figs. 1(a) and 1(b) for illustrations).

**Definition 3.** *The effective noise variance for the MMSE estimate of cB-AMP after  $t$  iterations is given by*

$$\sigma_{t+1}^2 = \lim_{M_R \rightarrow \infty} \frac{1}{M_R} \|\mathbf{r}^{t+1}\|_2^2 = N_0 + \beta \text{MSE}_t. \quad (10)$$

<sup>2</sup>The SE framework presented [37] focused on sparse signal recovery; we present SE framework for general prior distributions.

We note that a proof of (10) was given in [56, Lem. 4.1]. While  $\sigma_{t+1}^2$  corresponds to the effective noise variance (shown in Fig. 1(b)), the postulated output variance  $\gamma_{t+1}^2$  defined below corresponds to the *predicted* value of  $\sigma_{t+1}^2$  at iteration  $t$  of cB-AMP. If there is a mismatch in the noise variance  $N_0^{\text{post}} \neq N_0$ , then the postulated output variance  $\gamma_t^2$  differs from the actual noise variance  $\sigma_t^2$ , i.e.,  $\gamma_t^2 \neq \sigma_t^2$ .

**Definition 4.** *The postulated output variance of cB-AMP after  $t$  iterations is given by*

$$\begin{aligned} \gamma_{t+1}^2 &= \lim_{M_T \rightarrow \infty} N_0^{\text{post}} (1 + \tau^{t+1}) \\ &= N_0^{\text{post}} + \beta \lim_{M_T \rightarrow \infty} \frac{1}{M_T} \sum_{\ell=1}^{M_T} \mathbf{G}(\hat{s}_\ell^t + (\mathbf{h}_\ell^c)^H \mathbf{r}^t, N_0^{\text{post}} (1 + \tau^t)). \end{aligned} \quad (11)$$

We can now formulate the complex SE (cSE) framework with noise variance mismatch for cB-AMP. The complex SE framework was proven rigorously in [29]; for completeness, we resort to a heuristic derivation of the proof in Appendix D.

**Theorem 1.** *Suppose the entries of  $\mathbf{s}_0$  are i.i.d.  $p(\mathbf{s}_0) \sim \prod_{\ell=1}^{M_T} p(s_{0\ell})$  and the entries of the MIMO system matrix  $\mathbf{H}$  satisfy (A2). Let  $\mathbf{n} \sim \mathcal{CN}(\mathbf{0}_{M_R \times 1}, N_0 \mathbf{I}_{M_R})$  and  $F: \mathbb{C} \rightarrow \mathbb{C}$  be a pseudo-Lipschitz function as defined in [29, Sec. 1.1, Eq. 1.5]. Assume the large-system limit and that the postulated noise variance is  $N_0^{\text{post}}$ . Then, the effective noise variance  $\sigma_{t+1}^2$  in (10) and postulated output variance  $\gamma_{t+1}^2$  in (11) of cB-AMP in iteration  $t$  are given by the following coupled recursion:*

$$\sigma_{t+1}^2 = N_0 + \beta \Psi(\sigma_t^2, \gamma_t^2), \quad (12)$$

$$\gamma_{t+1}^2 = N_0^{\text{post}} + \beta \Phi(\sigma_t^2, \gamma_t^2). \quad (13)$$

*The MSE function  $\Psi$  and variance function  $\Phi$  are defined by*

$$\Psi(\sigma_t^2, \gamma_t^2) = \mathbb{E}_{S,Z} \left[ |F(S + \sigma_t Z, \gamma_t^2) - S|^2 \right], \quad (14)$$

$$\Phi(\sigma_t^2, \gamma_t^2) = \mathbb{E}_{S,Z} \left[ \mathbf{G}(S + \sigma_t Z, \gamma_t^2) \right], \quad (15)$$

*respectively, with  $S \sim p(S)$ ,  $Z \sim \mathcal{CN}(0, 1)$ . The recursion is initialized at  $t = 1$  with*

$$\sigma_1^2 = N_0 + \beta \text{Var}_S[S] \quad \text{and} \quad \gamma_1^2 = N_0^{\text{post}} + \beta \text{Var}_S[S].$$

We note that the MSE function  $\Psi(\sigma^2, \sigma^2)$  is identical to the ‘‘mmse(snr)’’ function in [3], [54], [57], [58] with the relation  $\text{snr} = 1/\sigma^2$  used to derive the relationship between the mutual information and the MSE function. We also note that the MSE of cB-AMP at iteration  $t$  as

defined in (9) is equivalent to  $\Psi(\sigma_t^2, \gamma_t^2)$  in the large-system limit. Theorem 1 implies that the effective noise variance of cB-AMP  $\sigma^2$  can be predicted exactly by the variance of a *single* random variable mixed with additive Gaussian noise in the large-system limit. If  $N_0 = N_0^{\text{post}}$ , then we obtain the following result.

**Corollary 2.** *Let  $N_0^{\text{post}} = N_0$  in Theorem 1. Then (12) is identical to (13), and the cSE reduces to the following recursion:*

$$\sigma_{t+1}^2 = N_0 + \beta\Psi(\sigma_t^2, \sigma_t^2). \quad (16)$$

The proof of Corollary 2 follows from the fact that the MSE equals to the conditional variance, i.e.,  $\Phi(\sigma_t^2, \sigma_t^2) = \Psi(\sigma_t^2, \sigma_t^2)$ . We note that Corollary 2 corresponds to the cSE derived originally in [37] in absence of noise-variance mismatch. Furthermore, for real-valued systems, Corollary 2 coincides with the original SE framework in [28], [30]. In Section IV-D, we will rely on cSE to analyze the performance and complexity of LAMA. In what follows, we assume that there is no mismatch in the prior distribution—this case was studied in [59].

### III. LAMA: LARGE-MIMO DETECTION USING CB-AMP

We now derive the LAMA algorithm. We specify the missing aspects of the large-MIMO system model and detail the LAMA algorithm along with the corresponding cSE framework.

#### A. Large MIMO and Optimal Data Detection

We consider a communication system in which the entries  $s_\ell$ ,  $\ell = 1, \dots, M_T$ , of the transmit data vector  $\mathbf{s}$  are taken from a finite constellation set  $\mathcal{O} = \{a_j : j = 1, \dots, |\mathcal{O}|\}$  with points  $a_j$  chosen, from e.g., a pulse amplitude modulation (PAM), phase-shift keying (PSK), or quadrature amplitude modulation (QAM) alphabet. We assume i.i.d. priors  $p(\mathbf{s}) = \prod_{\ell=1}^{M_T} p(s_\ell)$ , with the following distribution for each transmit symbol  $s_\ell$ :

$$p(s_\ell) = \sum_{a \in \mathcal{O}} p_a \delta(s_\ell - a). \quad (17)$$

Here,  $p_a$  is the (known) prior probability of each constellation point  $a \in \mathcal{O}$  and  $\delta(\cdot)$  is the Dirac delta distribution; for uniform priors we have  $p_a = 1/|\mathcal{O}|$ .

The vector  $\mathbf{s}_0$  is transmitted through a MIMO channel as in (1). We assume perfect knowledge of the MIMO system matrix  $\mathbf{H}$  at the receiver and the noise vector  $\mathbf{n}$  to be i.i.d. circularly

complex Gaussian with variance  $N_0$  per complex entry. For these assumptions, the individually optimal (IO) data-detection problem in [2], [3] is given by

$$s_\ell^{\text{IO}} = \arg \max_{\tilde{s}_\ell \in \mathcal{O}} \sum_{\tilde{\mathbf{s}}_\ell \in \mathcal{O}_\ell^{(M_T-1)}} \exp\left(-\frac{\|\mathbf{y} - \mathbf{H}\tilde{\mathbf{s}}\|^2}{N_0} + \log p(\tilde{\mathbf{s}})\right), \quad (18)$$

where  $\mathcal{O}_\ell^{(M_T-1)}$  stands for the subset of  $\mathcal{O}^{M_T}$  that excludes the  $\ell$ th entry and  $\tilde{\mathbf{s}}_\ell \in \mathcal{O}_\ell^{(M_T-1)}$  is a  $M_T - 1$  dimensional vector from this subset.

The detection problem in (18) is of combinatorial nature and requires prohibitive complexity in systems with large  $M_T$  [60]–[62]. We note that IO data detection achieves the minimum probability of symbol errors (see [60, Sec. 4.1] for a detailed discussion). While computationally efficient algorithms exist for small-scale MIMO systems (up to about eight transmit streams), such as sphere-decoding (SD) based methods [63]–[65], their average computational complexity still scales exponentially in  $M_T$  [61], [62].<sup>3</sup> Consequently, such methods are not suitable for large MIMO systems. In order to enable data detection for such systems, a variety of sub-optimal algorithms have been proposed in the past; see, e.g., [10], [66]–[70] and the references therein.

Instead of solving the IO problem in (18) directly, we first compute the marginalized distribution  $p(s_\ell | \mathbf{y}, \mathbf{H})$  using cB-AMP as in Algorithm 1. Once we obtain the marginalized distribution  $p(s_\ell | \mathbf{y}, \mathbf{H})$ ,  $\ell = 1, \dots, M_T$ , the IO data-detection problem is transformed in an entry-wise data detection problem that can be solved at low complexity.

### B. Derivation of the LAMA Algorithm

With the prior distribution in (17), we can write the posterior distribution (5) for the transmit symbol  $s_\ell$  as

$$f(s_\ell | \hat{s}_\ell, \tau) = \frac{1}{Z(\hat{s}_\ell, \tau)} \exp\left(-\frac{|s_\ell - \hat{s}_\ell|^2}{\tau}\right) \sum_{a \in \mathcal{O}} p_a \delta(s_\ell - a). \quad (19)$$

Since the normalization constant  $Z(\hat{s}_\ell, \tau)$  is chosen so that  $\int_{\mathcal{C}} f(s_\ell | \hat{s}_\ell, \tau) \mathbf{d}s_\ell = 1$ , we have

$$Z(\hat{s}_\ell, \tau) = \sum_{a \in \mathcal{O}} p_a \exp\left(-\frac{1}{\tau} |\hat{s}_\ell - a|^2\right),$$

<sup>3</sup>In the case of BPSK transmission, soft-input soft-output MAP detectors, such as the one in [65], can exactly solve the IO problem at low average computational complexity for a small number of transmit streams  $M_T$ . For higher-order modulation schemes, no known method exists to solve (18) at low complexity.

which enables us to write the message mean in (6) as follows

$$\begin{aligned} F(\hat{s}_\ell, \tau) &= \int_{\mathbb{C}} s_\ell f(s_\ell | \hat{s}_\ell, \tau) ds_\ell \\ &= \frac{\sum_{a \in \mathcal{O}} a p_a \exp\left(-\frac{1}{\tau} |\hat{s}_\ell - a|^2\right)}{\sum_{a' \in \mathcal{O}} p_{a'} \exp\left(-\frac{1}{\tau} |\hat{s}_\ell - a'|^2\right)} = \sum_{a \in \mathcal{O}} w_a(\hat{s}_\ell, \tau) a, \end{aligned} \quad (20)$$

where we use the shorthand notation

$$w_a(\hat{s}_\ell, \tau) = \frac{p_a \exp\left(-\frac{1}{\tau} |\hat{s}_\ell - a|^2\right)}{\sum_{a' \in \mathcal{O}} p_{a'} \exp\left(-\frac{1}{\tau} |\hat{s}_\ell - a'|^2\right)}.$$

The message variance  $G$  defined in (7) is given by

$$G(\hat{s}_\ell, \tau) = \int_{\mathbb{C}} |s_\ell|^2 f(s_\ell | \hat{s}_\ell, \tau) ds_\ell - |F(\hat{s}_\ell, \tau)|^2,$$

which can be simplified to

$$G(\hat{s}_\ell, \tau) = \sum_{a \in \mathcal{O}} w_a(\hat{s}_\ell, \tau) |a - F(\hat{s}_\ell, \tau)|^2. \quad (21)$$

The final step in the derivation of LAMA involves a simplification of the partial derivatives of (8) in Algorithm 1. The result is summarized by Lemma 2 with proof given in Appendix E.

**Lemma 2** (Message variance of the LAMA algorithm). *Suppose that the assumptions of Algorithm 1 hold, and the mean  $F(\hat{s}_\ell, \tau)$  as well as the variance  $G(\hat{s}_\ell, \tau)$  functions are given by (20) and (21), respectively. Then, the message variance is given by:*

$$G(\hat{s}_\ell, \tau) = \frac{\tau}{2} [\partial_1 F^R + \partial_2 F^I](\hat{s}_\ell, \tau)$$

and cB-AMP leads to Algorithm 2.

With Lemma 2 and Algorithm 1, we arrive at the LAMA algorithm summarized next.

**Algorithm 2** (LAMA). *Suppose that  $\mathbf{H}$  satisfies (A1) and [30, Lem. 5.56] holds. Then, the LAMA algorithm is given by following procedure*

$$\mathbf{z}^t = \hat{\mathbf{s}}^t + \mathbf{H}^H \mathbf{r}^t$$

$$\hat{\mathbf{s}}^{t+1} = \mathbf{F}(\mathbf{z}^t, N_0^{\text{post}}(1 + \tau^t)) \quad (22)$$

$$\tau^{t+1} = \frac{\beta}{N_0^{\text{post}}} \langle G(\mathbf{z}^t, N_0^{\text{post}}(1 + \tau^t)) \rangle \quad (23)$$

$$\mathbf{r}^{t+1} = \mathbf{y} - \mathbf{H} \hat{\mathbf{s}}^{t+1} + \frac{\tau^{t+1}}{1 + \tau^t} \mathbf{r}^t \quad (24)$$

for each iteration  $t = 1, 2, \dots$ . The LAMA algorithm is initialized at iteration  $t = 1$  with  $\hat{\mathbf{s}}^t = \mathbb{E}_S[S]\mathbf{1}_{M_T \times 1}$ ,  $S \sim p(S)$ ,  $\mathbf{r}^t = \mathbf{y} - \mathbf{H}\hat{\mathbf{s}}^t$ , and  $\tau^t = \beta \text{Var}[S]/N_0^{\text{post}}$ .

The main difference between the cB-AMP in Algorithm 1 and LAMA in Algorithm 2 is that the update in (8) for cB-AMP is simplified to (24) for LAMA and we utilize the prior distribution  $p(S)$  to initialize the algorithm. We note that LAMA as summarized in Algorithm 2 makes use of the postulated noise variance  $N_0^{\text{post}}$ ; this allows us not only to model a mismatch in the noise variance, but also enables us to perform IO detection and matched filter (MF) data detection solely by selecting appropriate values for  $N_0^{\text{post}}$ ; see Section III-D.

### C. LAMA Decouples Large-MIMO Systems

We now show that LAMA decouples a MIMO system into a set of parallel and independent AWGN channels with identical noise variance in the large system limit (cf. Figs. 1(a) and 1(b)). First, we discuss the outputs of LAMA: (i) the Gaussian output vector  $\mathbf{z}^t$ , (ii) the postulated variance  $N_0^{\text{post}}(1 + \tau^t)$ , and (iii) the non-linear MMSE output vector  $\hat{\mathbf{s}}^t$ .

(i) *Gaussian output vector  $\mathbf{z}^t$* : In each iteration  $t$ , cB-AMP computes the marginal distribution for  $s_\ell$  for  $\ell = 1, \dots, M_T$ , which corresponds to a Gaussian distribution centered around the original signal  $s_{0\ell}$  with variance  $\sigma_{t+1}^2$ . These properties on  $\mathbf{z}^t$  follow from Theorem 1, which shows that  $\mathbf{z}^t = \hat{\mathbf{s}}^t + \mathbf{H}^H \mathbf{r}^t$  is distributed according to  $\mathcal{CN}(s_0, \sigma_t^2 \mathbf{I}_{M_T})$  in the large-system limit [29], [56]. Therefore, the input–output relation for each transmit stream  $z_\ell^t = \hat{s}_\ell^t + (\mathbf{h}_\ell^c)^H \mathbf{r}_\ell^t$  is equivalent to the following single-input single-output AWGN channel:

$$z_\ell^t = s_{0\ell} + n_\ell^t. \quad (25)$$

Here,  $s_{0\ell}$  is the transmitted signal and  $n_\ell^t \sim \mathcal{CN}(0, \sigma_t^2)$  is AWGN with effective noise variance  $\sigma_t^2$  per complex entry. Since  $p(z_\ell^t | s_{0\ell}) \sim \mathcal{CN}(s_{0\ell}, \sigma_t^2)$ , the posterior distribution of (25) as defined in (19) is given by  $f(s_{0\ell} | z_\ell^t, \sigma_t^2)$ . An immediate consequence of these properties is the fact that LAMA decouples the MIMO system (cf. Fig. 1(b)). We note that the decoupling behavior of LAMA was observed for posterior mean estimators (PMEs) in randomly spread CDMA systems [3], [60] for which no practical data detection algorithm was given.

(ii) *Postulated output variance  $N_0^{\text{post}}(1 + \tau^t)$* : In the large-system limit, there exist two noise variances: effective noise variance  $\sigma_t^2$  from Definition 3 and the postulated output variance  $\gamma_t^2$  from Definition 4. We note that  $N_0^{\text{post}}(1 + \tau^t) \rightarrow \gamma_t^2$  in the large-system limit. We clarify the difference between the two quantities below.

The effective noise variance  $\sigma_t^2$  is the *true* noise variance in (25), whereas the postulated output variance  $\gamma_t^2$  is the estimate for  $\sigma_t^2$  each iteration  $t$ . The postulated output variance  $\gamma_t^2$  is used as an input to the posterior mean function  $F$  (see (22) and Figs. 3(a) and 3(b)) to the Gaussian vector  $\mathbf{z}^t$  to obtain the MMSE estimate  $\hat{\mathbf{s}}^{t+1}$ . Therefore, when the exact value of  $\sigma_t^2$  is unknown at the receiver, a possible performance mismatch can result in using an incorrect value  $\gamma_t^2$  for obtaining the MMSE estimate. The cSE framework shown in Theorem 1 enables us to analyze the performance loss due to such a (possible) mismatch in the noise variance  $N_0^{\text{post}}$  *exactly*.

If there is no mismatch in the postulated noise variance, we have  $\sigma_t^2 = \gamma_t^2$  by Corollary 2 and hence, the correct noise variance statistic is used for the MMSE estimate in (22) every iteration. However, if  $N_0^{\text{post}} \neq N_0$ , then  $\sigma_t^2 \neq \gamma_t^2$ , and therefore, LAMA applies the MMSE estimate on the Gaussian vector  $\mathbf{z}^t$  according to an incorrect statistic, which may cause LAMA to converge to an incorrect solution. To illustrate how LAMA may converge to an incorrect solution, consider the case where  $N_0 = 0$ , and  $N_0^{\text{post}} \rightarrow \infty$ . In this case,  $\mathbf{z}^t$  corresponds to the MF detector; see Section III-D for more details.

(iii) *Non-linear MMSE output vector  $\hat{\mathbf{s}}^{t+1}$* : The non-linear MMSE output vector  $\hat{\mathbf{s}}^{t+1}$  is given by  $\hat{\mathbf{s}}^{t+1} = F(\mathbf{z}^t, N_0^{\text{post}}(1 + \tau^t))$  in (20), which can be seen as a conditional mean of the Gaussian output vector  $\mathbf{z}^t$  for the postulated output variance  $N_0^{\text{post}}(1 + \tau^t)$ . The non-linear MMSE output vector  $\hat{\mathbf{s}}^{t+1}$  is identical to the PME [3], where each  $\ell$ th output of PME is obtained by the expectation with respect to the conditional distribution  $f(s_\ell | z_\ell^t, N_0^{\text{post}}(1 + \tau^t))$  in (19).<sup>4</sup> The equivalence of LAMA and the equivalent AWGN relation for the non-linear MMSE estimate is shown in Fig. 3. In Fig. 3(a), the quantity  $\hat{\mathbf{s}}^{t+1}$  is the non-linear MMSE estimate with the postulated noise variance  $N_0^{\text{post}}(1 + \tau^t)$ . In the large system limit, the input-output relation for each stream  $\ell$  is an AWGN channel in Fig. 3(b) with equivalent variance  $\sigma_t^2$  and the postulated variance  $\gamma_t^2$ .

#### D. LAMA and MF Data Detection

Since LAMA decouples the MIMO system, data detection reduces to element-wise hard decisions for each entry in  $\mathbf{z}^t$  subject to the postulated output variance  $N_0^{\text{post}}(1 + \tau^t)$  as

$$\hat{s}_\ell^t = \arg \max_{s_\ell \in \mathcal{O}} f(s_\ell | z_\ell^t, N_0^{\text{post}}(1 + \tau^t)). \quad (26)$$

<sup>4</sup>The conditional distribution  $f(s_\ell | z_\ell^t, N_0^{\text{post}}(1 + \tau^t))$  is called “retro-channel” in [3].



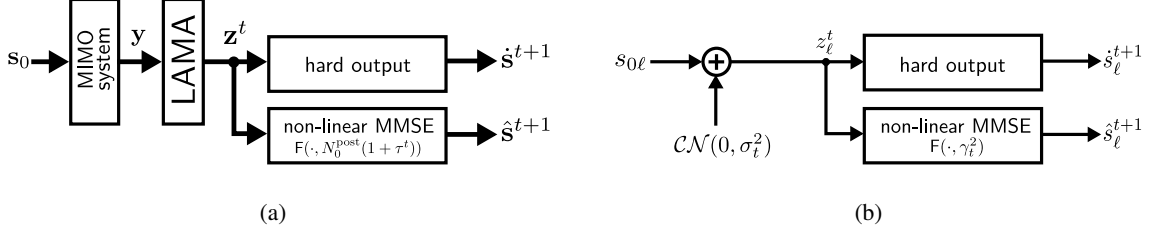


Fig. 3. The system with LAMA and its outputs (a) and the statistically-equivalent decoupled AWGN system as seen at the output of LAMA (b). LAMA generates a Gaussian output  $\mathbf{z}^t$  and a non-linear MMSE estimator output  $\hat{\mathbf{s}}^{t+1}$ . Hard-output estimates  $\hat{s}^{t+1}$  are generated via (26). In the large system limit, LAMA decouples the MIMO system into independent, parallel AWGN channels with equivalent output noise variance  $\sigma_t^2$ .

By setting the postulated noise variance  $N_0^{\text{post}}$ , LAMA can perform IO and MF data detection. In particular, (i) for  $N_0^{\text{post}} = N_0$ , LAMA corresponds to the IO detector and (ii) for  $N_0^{\text{post}} \rightarrow \infty$ , LAMA corresponds to the MF detector. These two “operation modes” are detailed next.

(i): Consider  $N_0^{\text{post}} = N_0$ . From Corollary 2, we have that the equivalent output noise variance and the postulated noise variance are equal, which implies  $\sigma_t^2 = \gamma_t^2$  in the large-system limit. Since there is no noise variance mismatch, the output (26) achieves the same error-rate performance as the IO data detector which in (18) given certain conditions are met; see Section IV-E for precise optimality conditions.

(ii): By letting  $N_0^{\text{post}} \rightarrow \infty$ , it was shown in [3, Eq. (12)] that the output of the non-linear MMSE estimator (20) corresponds to the MF output for real-valued signals with  $\mathbb{E}[S] = 0$ . We now provide conditions for which LAMA with  $N_0^{\text{post}} \rightarrow \infty$  performs MF data detection for arbitrary system ratios  $\beta$ . The proof of the following Lemma is given in Appendix F.

**Lemma 3.** Fix the constellation set  $\mathcal{O}$ , and let  $S \sim p(S)$ . If  $\mathbb{E}_S[S] = 0$ , then as  $N_0^{\text{post}} \rightarrow \infty$ , the Gaussian output at every iteration  $t = 1, 2, \dots$ , from LAMA corresponds to the MF output:

$$\lim_{N_0^{\text{post}} \rightarrow \infty} \mathbf{z}^t = \mathbf{H}^H \mathbf{y}.$$

If  $\mathbb{E}_S[\text{Re}\{S\}\text{Im}\{S\}] = \mathbb{E}_S[S|S|^2] = 0$ , then, as  $N_0^{\text{post}} \rightarrow \infty$ , the scaled version of the non-linear MMSE estimate also corresponds to the MF output:

$$\lim_{N_0^{\text{post}} \rightarrow \infty} \frac{N_0^{\text{post}}}{E_s} \hat{\mathbf{s}}^t = \mathbf{H}^H \mathbf{y}.$$

### E. LAMA in the Massive MU-MIMO Limit

We now study the properties of LAMA in the massive MU-MIMO limit, where we fix the number of streams (or layers)  $M_T$  and let the number of BS antennas  $M_R \rightarrow \infty$ . As shown in [4], [5], MF data detection is optimal in such scenarios. The following Lemma reveals that LAMA corresponds to the MF detector in the massive MU-MIMO limit; a proof is given in Appendix G.

**Lemma 4.** *Assume that  $\mathcal{O}$  is fixed and let  $N_0^{\text{post}} \geq 0$ . Then, for  $\beta \rightarrow 0$ , the Gaussian output  $\mathbf{z}^t$  of LAMA corresponds to the MF data detector, i.e.,  $\mathbf{z}^t = \mathbf{H}^H \mathbf{y}$ , for all  $t \geq 1$ . Furthermore, the effective noise variance is  $\sigma_t^2 = N_0$  for all  $t \geq 1$ .*

This result is in accordance with [4], [5] and implies that a simple one-shot algorithm (performing a single iteration) is sufficient to perform IO data detection in the massive MU-MIMO limit. Furthermore, LAMA decouples the MIMO system into parallel and independent AWGN channels with variance  $\sigma_t^2 = N_0$  (see Fig. 1(a) and Fig. 1(b)) in every iteration. We emphasize that LAMA can be used in more-realistic massive MU-MIMO systems, i.e., where the number of BS antennas is finite. As we will show in Section V-B, LAMA quickly converges and provides near-optimal performance for realistic massive MU-MIMO antenna configurations.

## IV. OPTIMALITY OF LAMA

We now provide exact conditions for which LAMA achieves the performance of the IO data detector. We furthermore study the noiseless case in which LAMA is able to perform error-free data recovery.

### A. Existing Results of IO and Multiuser Detection in Large MIMO Systems

An spectral efficiency analysis of IO data detection in large systems with BPSK was presented by Tanaka in [16]. These results were generalized to arbitrary constellation sets in [3]. Under the assumption that replica method is correct, Guo and Verdú showed in [3] that by using PME, the multi-user channel in the large-system limit decouples into an AWGN channel for each transmit stream, where the noise is amplified by a factor  $\eta^{-1}$  due to the interference of other streams. The factor  $\eta \in (0, 1)$ , known as the multi-user efficiency, can be computed exactly by solving the following coupled equations for  $\eta$  and  $\xi$ :

$$N_0/\eta = N_0 + \beta \mathbb{E}_{S,Z} \left[ \left| \mathbf{F} \left( S + \sqrt{N_0/\eta} Z, N_0/\xi \right) - S \right|^2 \right], \quad (27)$$

$$N_0/\xi = N_0^{\text{post}} + \beta \mathbb{E}_{S,Z} \left[ \mathbf{G} \left( S + \sqrt{N_0/\eta} Z, N_0/\xi \right) \right]. \quad (28)$$

Here, the functions  $\mathbf{F}$  and  $\mathbf{G}$  depend on constellation set  $\mathcal{O}$  as in (6) and (7), respectively.

We note that the performance of IO data detection corresponds to the case with  $N_0 = N_0^{\text{post}}$ . In this case, the right-hand side of (28) is equal to (28), and therefore,  $\eta = \xi$ . Thus, the multi-user efficiency  $\eta$  is given by a single fixed-point equation

$$N_0/\eta = N_0 + \beta \mathbb{E}_{S,Z} \left[ \left| \mathbf{F} \left( S + \sqrt{N_0/\eta} Z, N_0/\eta \right) - S \right|^2 \right]. \quad (29)$$

If there exist multiple fixed points to (27) and (28), we pick the tuple  $(\eta, \xi)$  that minimizes the so-called ‘‘free energy’’ (as done in [3, Sec. 2-D]) given by:

$$\begin{aligned} \mathcal{F} = & \int_{\mathbb{C}} p(z, N_0/\eta) \log_2 p(z, N_0/\xi) dz \\ & + \frac{1}{\beta} ((\xi - 1) \log_2 e - \log_2 \xi) + \log_2 \frac{\xi}{\pi} - \frac{\xi}{\eta} \log_2 e \\ & + \frac{N_0^{\text{post}}}{\beta N_0} \frac{\xi}{\eta} (\eta - \xi) \log_2 e + \frac{1}{\beta} \log_2(2\pi) + \frac{\xi}{\eta\beta} \log_2 e, \end{aligned} \quad (30)$$

where the term  $p(z, x)$  in (30) is obtained by marginalizing the joint distribution  $p(z, x|s) \sim \mathcal{CN}(s, x)$  with respect to the prior distribution  $s \sim p(s)$ , i.e.,  $p(z, x) = \int_{\mathbb{C}} p(z, x|s)p(s)ds$ .

We note that the aforementioned results rely on the replica method, which build on the replica assumptions [3], [16]. Montanari and Tse in [24] proposed an alternative approach to prove Tanaka’s results in [16] up to certain system ratios  $\beta$  for BPSK systems. Instead of directly analyzing a dense MIMO system matrix, Montanari and Tse first introduce a ‘‘sparse signature’’ scheme, in which only a sparse subset of the channel matrix is active. For this system, the performance of belief propagation (BP) can be analyzed via density evolution. Once the density evolution expressions were established in the large-system limit, one can ‘‘densify’’ the MIMO system matrix to ensure that the each entry is distributed (A1); we shall refer to this setup as *large-sparse* limit [71]. By doing so, one recovers Tanaka’s results derived under the replica method without relying on the replica assumptions. The analysis of BPSK systems using this sparse signature scheme has been generalized to arbitrary prior input distributions in [25], [26], [71]. Not surprisingly, these results agree with the replica results [3] when the fixed-point  $\eta$  to (29) is unique. In addition, in [71], Wang and Guo showed that BP is equivalent to element-wise MAP estimation, and the detection performance of the BP is identical to that given by a AWGN system with noise amplified by  $\eta^{-1}$  obtained in (29).

### B. Fixed Points of LAMA

Before we provide exact optimality conditions for LAMA, we highlight that under Theorem 1, as  $t \rightarrow \infty$  the cSE converges to the following fixed-point equations: for  $N_0 = N_0^{\text{post}}$ , we have

$$\sigma_{\text{IO}}^2 = N_0 + \beta\Psi(\sigma_{\text{IO}}^2, \sigma_{\text{IO}}^2), \quad (31)$$

whereas for  $N_0^{\text{post}} \neq N_0$ , we have

$$\sigma_{\text{m}}^2 = N_0 + \beta\Psi(\sigma_{\text{m}}^2, \gamma_{\text{m}}^2) \quad \text{and} \quad \gamma_{\text{m}}^2 = N_0^{\text{post}} + \beta\Phi(\sigma_{\text{m}}^2, \gamma_{\text{m}}^2). \quad (32)$$

As mentioned above, the fixed-point equation for LAMA in (31) and (32) corresponds to the fixed-point equations for IO data detection in (29), and (27) and (28), respectively, with  $\sigma_{\text{m}}^2 = N_0/\eta$  and  $\gamma_{\text{m}}^2 = N_0/\xi$ .

In general, the above fixed-point equations may have multiple solutions. In the case of a unique fixed point, then LAMA *always* recovers the solution with the minimal effective noise variance  $\sigma^2$  regardless of initialization, and thus, achieves the same error-rate performance as IO data detection (see Section IV-C for the details). In the case of such non-unique fixed points, Guo and Verdú choose the solution that minimizes free-energy<sup>5</sup> given in (30), whereas the fixed point obtained by LAMA depends on the initialization<sup>6</sup> of the algorithm and thus, we cannot expect it to converge to the same fixed point that minimizes the free-energy (30). We note that depending on the initialization of LAMA presented in Algorithm 2, LAMA converges to the fixed-point solution with the largest effective noise variance  $\sigma^2$  in (31) and (32), respectively. Therefore, if there are multiple fixed points to (31), then LAMA is, in general, sub-optimal and does not necessarily converge to the fixed-point solution with minimal free-energy.

Before we delve into the optimality analysis of LAMA, we note that the fixed-point analysis for LAMA with noise mismatch is more involved as it requires finding fixed points for the coupled fixed-point equations in (32). Hence, we focus on the case  $N_0 = N_0^{\text{post}}$ .

### C. When Does LAMA Achieve the Same Performance as IO Data Detector?

We note that the performance of LAMA (in the large-system limit) is fully described by the SE framework. However, characterizing the performance of the IO data detector is a non-trivial

<sup>5</sup>The solution that minimizes the free energy in (30) is equivalent to the thermodynamically dominant solution in statistical physics [3], [16].

<sup>6</sup>Convergence to another fixed-point solution is possible if LAMA is initialized sufficiently close to such a fixed point [72].

task. Although an analysis via the replica method [3] was recently proved to be correct under mild assumptions [73], a verification of the assumptions still requires extensive work for each prior distribution. Therefore, to establish optimality of LAMA, we first introduce an additional assumption to characterize the performance of the IO data detector, and then show that under this assumption, LAMA achieves the same data detection performance as the IO data detector.

We define a specific example of a large-sparse limit that will be used for our analysis of LAMA. The general definition of large-sparse limit is provided in [71].

**Definition 5.** *We define the large-sparse limit as the following procedure: First, start by defining a binary-valued matrix  $\mathbf{B} \in \{0, 1\}^{M_R \times M_T}$ . Pick a constant  $\Gamma \leq M_T$  and generate each entry  $B_{k,\ell}$  as an i.i.d. Bernoulli random variable with probability  $\Gamma/M_T$ . Define a normalization constant  $\Gamma_\ell = \sum_{k=1}^{M_R} B_{k,\ell}$  for each  $\ell = 1, \dots, M_T$ . Then, generate the channel matrix  $\mathbf{H}$  with each entry being i.i.d.  $H_{k,\ell} \in \mathcal{CN}(0, 1/\Gamma_\ell)$  if  $B_{k,\ell} = 1$  and 0 otherwise. Based on this construction of  $\mathbf{H}$  for a fixed  $\Gamma$ , we define the large-sparse limit when we first let  $M_R, M_T \rightarrow \infty$  with  $M_T/M_R = \beta$ . Then, we let  $\Gamma \rightarrow \infty$ .*

We note that the large-system limit corresponds to the case when we first set  $\Gamma = M_T$  and then let  $M_R, M_T \rightarrow \infty$  with  $M_T/M_R = \beta$ . However, we will assume that we first fix a constant  $\Gamma < M_T$ , and then let  $M_R, M_T \rightarrow \infty$ ; this formulation of the large-sparse limit is needed to prevent the factor graph for the input-output relation in (1) from having short cycles [71]. We need an additional assumption to establish optimality of LAMA. We assume that exchanging the order of the large-system limit still holds true for cSE:

(A3) We assume that cSE for LAMA remains valid in the large-sparse limit.

With Definition 5 and (A3), we will now establish optimality of LAMA in two parts. First, we show that in the large-sparse limit, BP achieves the same performance as the IO data detector and the input-output relation is asymptotically decoupled into AWGN channels with equal decoupled noise variance. Second, we show that LAMA achieves the same noise variance as that given by BP using state evolution. Since the input-output relation is decoupled into AWGN channels and LAMA achieves the lowest (unique) decoupled noise variance, LAMA achieves the same detection performance as the IO data detector. We show the first part by [71, Thm. 4]:

**Theorem 3.** *Assume the large-sparse limit and the system ratio  $\beta_{BP}$  is chosen such that the fixed-point solution of BP  $\eta_{BP}$  to (29) is unique. Then, BP achieves the same performance as the*

*IO data detector. In addition, the posterior distribution of each user after BP converges to that given by an AWGN channel with variance  $N_0/\eta_{\text{BP}}$ .*

Theorem 3 shows that in the large-sparse limit and for unique fixed points, one can use BP to achieve the same performance as IO data detector. The proof in [71, Sec. V] uses a sandwiching argument between genie-aided BP and classical BP to achieve IO performance. Interestingly, the posterior distribution of each transmit stream after BP converges to that given by an AWGN channel. In addition, the noise variance of the equivalent AWGN channel can be characterized by solving a fixed-point equation (29); this fixed-point equation coincides exactly to that given by the replica method shown in [3]. Now that we have shown that BP achieves IO performance and characterized the decoupling of AWGN, we now establish optimality of LAMA.

**Corollary 4.** *Assume the large-system limit and  $\beta_{\text{LAMA}} = \beta_{\text{BP}}$  from Theorem 3. Then, LAMA decouples the MIMO system into parallel AWGN channels with variance  $\sigma_{\text{IO}}^2$ , which is a unique fixed-point solution to (31) with  $\sigma_{\text{IO}}^2 = N_0/\eta_{\text{BP}}$  from Theorem 3.*

The proof of Corollary 4 follows from first noting that (29) and (31) are equal. Hence, since  $\beta_{\text{LAMA}} = \beta_{\text{BP}}$ , LAMA has a unique fixed-point solution to (31) given by  $\sigma_{\text{IO}}^2$  which is equivalent to  $N_0/\eta_{\text{BP}}$ . Since LAMA decouples the MIMO system into parallel AWGN channels [29] and the decoupled variances are equal, LAMA achieves the same performance as the IO data detector. In Section IV-E, we provide conditions for which there is exactly one (unique) fixed point with minimum effective noise variance  $\sigma^2$ .

#### D. Exact Recovery Thresholds (ERTs)

We start by analyzing LAMA in a noiseless setting and for  $N_0 = N_0^{\text{post}} = 0$ . We provide sharp bounds on the system ratio  $\beta = M_{\text{T}}/M_{\text{R}}$ , which guarantee exact recovery of an unknown transmit signal  $\mathbf{s}_0$  in the large-system limit. We show that if  $\beta < \beta_{\mathcal{O}}^{\text{max}}$ , where  $\beta_{\mathcal{O}}^{\text{max}}$  is the so-called *exact recovery threshold (ERT)*, then LAMA perfectly recovers  $\mathbf{s}_0$ . Note that the ERT depends on the constellation  $\mathcal{O}$  and resembles to the phase-transition behavior observed in sparse signal recovery [48], [74], [75]; the key difference is that LAMA operates with dense vectors.

We will show in Theorem 5 that if  $\beta < \beta_{\mathcal{O}}^{\text{max}}$ , there exists a unique fixed point at  $\sigma^2 = 0$  to the fixed-point equation in (31). The unique fixed point at  $\sigma^2 = 0$  implies that the effective noise variance output for the decoupled AWGN channel will be zero. Therefore, the output

from the non-linear MMSE estimate from LAMA will be  $F(s_0, \sigma^2) = s_0$  from (20), and hence LAMA perfectly recovers  $s_0$ . For  $\beta \geq \beta_{\mathcal{O}}^{\max}$ , perfect recovery cannot be guaranteed.<sup>7</sup> To make this behavior explicit, we need the following technical result with proof in Appendix H.

**Lemma 5.** *Fix the constellation set  $\mathcal{O}$  and let  $\text{Var}_S[S]$  be finite. Then, there exists a non-negative gap  $\sigma^2 - \Psi(\sigma^2, \sigma^2) \geq 0$  with equality if and only if  $\sigma^2 = 0$ . As  $\sigma^2 \rightarrow 0$ , we have MSE  $\Psi(\sigma^2, \sigma^2) \rightarrow 0$ ; as  $\sigma^2 \rightarrow \infty$ , we have the the MSE  $\Psi(\sigma^2, \sigma^2) \rightarrow \text{Var}_S[S]$ .*

For a finite value of  $\text{Var}_S[S]$ , Lemma 5 shows that we have  $\Psi(\sigma^2, \sigma^2) < \sigma^2$  for all  $\sigma^2 > 0$ . Now, suppose that for some  $\beta > 1$ ,  $\beta\Psi(\sigma^2, \sigma^2) < \sigma^2$  also holds for all  $\sigma^2 > 0$ . Then, as long as  $\beta > 1$  is not too large to also ensure  $\beta\Psi(\sigma^2, \sigma^2) < \sigma^2$ , for all  $\sigma^2 > 0$ , there will only be a *single* fixed point at  $\sigma^2 = 0$ . Therefore, LAMA is able to perfectly recover the original signal  $s_0$  by Theorem 1 since the unique fixed point at  $\sigma^2 = 0$  implies that  $\Psi(\sigma^2, \sigma^2) = 0$ . Leveraging the gap between  $\Psi(\sigma^2, \sigma^2)$  and  $\sigma^2$  will allow us to find the exact recovery threshold (ERT) of LAMA for values of  $\beta > 1$ . For the fixed (discrete) constellation  $\mathcal{O}$ , the largest value of  $\beta$  that ensures  $\beta\Psi(\sigma^2, \sigma^2) < \sigma^2$  is precisely the ERT.

**Definition 6.** *Fix  $\mathcal{O}$  and let  $N_0 = N_0^{\text{post}} = 0$ . Then, the exact recovery threshold (ERT) that enables perfect recovery by LAMA is defined by*

$$\beta_{\mathcal{O}}^{\max} = \min_{\sigma^2 \geq 0} \left\{ \left( \frac{\Psi(\sigma^2, \sigma^2)}{\sigma^2} \right)^{-1} \right\}. \quad (33)$$

We are now ready to establish perfect recovery with  $\beta_{\mathcal{O}}^{\max}$ ; the proof is given in Appendix I.

**Theorem 5.** *Let  $N_0 = N_0^{\text{post}} = 0$  and  $\mathbf{H}$  satisfy (A2). Fix the constellation  $\mathcal{O}$ . If  $\beta < \beta_{\mathcal{O}}^{\max}$ , then LAMA perfectly recovers  $s_0$  in (1) in the large-system limit.*

We emphasize that for a given constellation  $\mathcal{O}$ , the ERT  $\beta_{\mathcal{O}}^{\max}$  can be computed numerically from (33), where  $\Psi(\sigma^2, \sigma^2)$  is given by Theorem 1. We emphasize that the signal variance,  $\text{Var}_S[S]$  does not have an impact on the ERT as the MSE function  $\Psi(\sigma^2, \sigma^2)$  and  $\sigma^2$  both scale linearly with  $\text{Var}_S[S]$ . In Section IV-E, we extend our analysis to the noisy case.

<sup>7</sup>We assume the initialization as given in Algorithm 2. LAMA may recover the original signal for  $\beta \geq \beta_{\mathcal{O}}^{\max}$  if initialized sufficiently close to the optimal fixed point; see [72] for a discussion.

TABLE I  
SUMMARY OF (SUB-)OPTIMALITY REGIMES OF LAMA

	$\beta < \beta_{\mathcal{O}}^{\min}$	$\beta_{\mathcal{O}}^{\min} \leq \beta \leq \beta_{\mathcal{O}}^{\max}$	$\beta_{\mathcal{O}}^{\max} < \beta$
$N_0 < N_0^{\min}(\beta)$	<i>optimal</i>	<i>optimal</i>	suboptimal
$N_0^{\min}(\beta) \leq N_0 \leq N_0^{\max}(\beta)$	<i>optimal</i>	(sub-)optimal <sup>9</sup>	suboptimal
$N_0^{\max}(\beta) < N_0$	<i>optimal</i>	<i>optimal</i>	<i>optimal</i>

### E. Optimality Conditions for LAMA With Noise

We develop optimality conditions of LAMA in the presence of noise, and we focus on mismatch-free case as the associated optimality conditions allow for an elegant analysis.<sup>8</sup>

In the presence of noise ( $N_0 > 0$ ), exact recovery is no longer guaranteed. Nevertheless, if LAMA converges to a unique fixed-point, then we obtain the same error-rate performance as the IO data detector. In such situations, we call LAMA to be optimal. Furthermore, if multiple fixed-points exist, we call the fixed-point with minimum effective noise variance the *optimal fixed point*, whereas all other fixed points are called *suboptimal fixed points*.

In essence, there exist three different regimes for LAMA (see Table I), which depend on the system ratio  $\beta$ : (i) if  $\beta$  is smaller than the so-called *minimum recovery threshold* (MRT)  $\beta_{\mathcal{O}}^{\min}$ , then LAMA is *always* guaranteed to converge to the unique fixed point (with minimal  $\sigma^2$ ), i.e., the LAMA delivers IO data detection performance irrespective of the noise variance  $N_0$  (ii) if  $\beta$  is larger or equal to than the MRT, but smaller than or equal to the ERT, then multiple fixed points exist. In this case, optimality of LAMA depends on the noise variance  $N_0$ . If the noise variance  $N_0$  is *larger* than the so-called *maximum guaranteed noise variance*  $N_0^{\max}(\beta)$ , then LAMA converges to the unique fixed point. Similarly, if the noise variance  $N_0$  is strictly *smaller* than the so-called *minimum critical noise*  $N_0^{\min}(\beta)$ , then LAMA converges to the optimal fixed point. However, if  $N_0 \in [N_0^{\min}(\beta), N_0^{\max}(\beta)]$ , then LAMA converges, in

<sup>8</sup> The mismatch-free case requires us to identify all fixed points of (31), whereas mismatch case requires the identification of all fixed points to the *coupled* fixed-point equations in (32). A detailed analysis of optimality conditions for LAMA with noise variance mismatch is left for future work.

<sup>9</sup>For some constellations, there may exist intervals in  $[N_0^{\min}(\beta), N_0^{\max}(\beta)]$  where LAMA is still optimal; an example is shown in Fig. 4(d).



general, to a sub-optimal fixed point<sup>10</sup>. We also note that for some constellations, there may exist intervals in  $[N_0^{\min}(\beta), N_0^{\max}(\beta)]$  in which LAMA remains to be optimal. This behavior is shown in Fig. 4(d). Furthermore, as  $\beta \rightarrow \beta_{\mathcal{O}}^{\max}$ , the minimum critical noise  $N_0^{\min}(\beta) \rightarrow 0$ , which implies that LAMA is optimal when  $N_0 > N_0^{\max}(\beta)$ . (iii) If  $\beta$  exceeds the ERT, then LAMA is optimal if  $N_0 > N_0^{\max}(\beta)$ . For all other values of  $N_0$ , LAMA converges, in general, to a sub-optimal fixed point. In order to make these three regimes more explicit, we require the following definition.

**Definition 7.** Fix the constellation  $\mathcal{O}$  and let  $N_0^{\text{post}} = N_0$ . Then, the minimum recovery threshold (MRT)  $\beta_{\mathcal{O}}^{\min}$  is defined as follows:

$$\beta_{\mathcal{O}}^{\min} = \min_{\sigma^2 \geq 0} \left\{ \left( \frac{d\Psi(\sigma^2, \sigma^2)}{d\sigma^2} \right)^{-1} \right\}. \quad (34)$$

By the definition of the MRT, it is easy to observe that the fixed point of (31) is unique for all system ratios  $\beta < \beta_{\mathcal{O}}^{\min}$ , as  $\beta \frac{d\Psi(\sigma^2, \sigma^2)}{d\sigma^2} < 1$  for all values of  $\sigma^2$ . The following lemma establishes an intuitive relationship between MRT and ERT; the proof is given in Appendix J.

**Lemma 6.** *The MRT never exceeds the ERT.*

Lemma 6 shows that if the system ratio  $\beta$  is less than MRT, i.e.,  $\beta < \beta_{\mathcal{O}}^{\min}$ , then LAMA is not only optimal but also perfect recovery is possible in noiseless settings. We next define the minimum critical and maximum guaranteed noise variance,  $N_0^{\min}(\beta)$  and  $N_0^{\max}(\beta)$ , that determine boundaries for the optimality regimes when  $\beta \geq \beta_{\mathcal{O}}^{\min}$ .

**Definition 8.** Fix the system ratio  $\beta \in [\beta_{\mathcal{O}}^{\min}, \beta_{\mathcal{O}}^{\max}]$ . Then, the minimum critical noise variance  $N_0^{\min}(\beta)$  that ensures convergence to the optimal fixed-point is defined by

$$N_0^{\min}(\beta) = \min_{\sigma^2 \geq 0} \left\{ \sigma^2 - \beta \Psi(\sigma^2, \sigma^2) : \beta \frac{d\Psi(\sigma^2, \sigma^2)}{d\sigma^2} = 1 \right\}.$$

**Definition 9.** Fix the system ratio  $\beta \geq \beta_{\mathcal{O}}^{\min}$ . Then, the maximum guaranteed noise variance  $N_0^{\max}(\beta)$  that ensures convergence to the optimal fixed-point is defined by

$$N_0^{\max}(\beta) = \max_{\sigma^2 \geq 0} \left\{ \sigma^2 - \beta \Psi(\sigma^2, \sigma^2) : \beta \frac{d\Psi(\sigma^2, \sigma^2)}{d\sigma^2} = 1 \right\}.$$

<sup>10</sup>We note that LAMA can still be optimal if it was initialized close to the optimal fixed point [30], but we exclude this case from our analysis.

Note that as  $\beta \rightarrow \beta_{\mathcal{O}}^{\max}$ , the minimum critical noise decreases to  $N_0^{\min}(\beta) \rightarrow 0$ . To see this, consider the case when  $\beta = \beta_{\mathcal{O}}^{\max}$ , so that there exists a  $\sigma_*^2 > 0$  such that  $\beta_{\mathcal{O}}^{\max} \Psi(\sigma_*^2, \sigma_*^2) = \sigma_*^2$ . It is clear that  $\beta_{\mathcal{O}}^{\max} \frac{d\Psi(\sigma^2, \sigma^2)}{d\sigma^2} \Big|_{\sigma^2=\sigma_*^2} = 1$  and hence  $N_0^{\min}(\beta_{\mathcal{O}}^{\max}) = \sigma_*^2 - \beta_{\mathcal{O}}^{\max} \Psi(\sigma_*^2, \sigma_*^2) = 0$ .

Before we proceed with the analysis for optimality regimes of LAMA, we present Lemma 7 (with proof in Appendix K) that shows how the fixed-point  $\sigma^2$  decreases with  $N_0$  as  $N_0 \rightarrow 0$ .

**Lemma 7.** *Fix the constellation  $\mathcal{O}$  and let  $\beta < \beta_{\mathcal{O}}^{\max}$ . Denote  $\sigma^2$  as the largest fixed-point solution of LAMA with noise variance  $N_0$ . Then, as  $N_0 \rightarrow 0$ , we have  $\sigma^2 \rightarrow 0$ . In addition, we have  $\lim_{N_0 \rightarrow 0} \frac{\sigma^2}{N_0} = 1$ .*

Lemma 7 shows that not only the fixed-point solution  $\sigma^2$  of LAMA goes to 0 as  $N_0 \rightarrow 0$ , but also decreases linearly as  $\lim_{N_0 \rightarrow 0} \frac{\sigma^2}{N_0} = 1$ . We now proceed to the optimality regime analysis. We recall that all the zero-crossing points of the function

$$g(\sigma^2, \beta, N_0, \mathcal{O}) = N_0 + \beta \Psi(\sigma^2, \sigma^2) - \sigma^2 \quad (35)$$

correspond to all the fixed points of the cSE of LAMA. We will frequently refer to the function in (35) for our optimality analysis of LAMA.

Figure 4 illustrates our optimality analysis for a large MIMO system with QPSK. We plot the function (35) depending on the effective noise variance  $\sigma^2$  and for different system ratios  $\beta$ . The cases  $\beta < \beta_{\mathcal{O}}^{\min}$ ,  $\beta \in [\beta_{\mathcal{O}}^{\min}, \beta_{\mathcal{O}}^{\max}]$ , and  $\beta > \beta_{\mathcal{O}}^{\max}$  are shown in Fig. 4(a), Fig. 4(b), and Fig. 4(c), respectively. The special case of  $\beta = 1$  in the noiseless setting  $N_0 = 0$  for (35) corresponds to the solid blue line, along with the corresponding (unique) fixed point at the origin. In the following three paragraphs, we discuss the three operation regimes of LAMA.

(i)  $\beta < \beta_{\mathcal{O}}^{\min}$ : In this region, the cSE of LAMA always converges to the unique, optimal fixed point. For  $\beta < \beta_{\mathcal{O}}^{\min}$ , the slope of (35) is strictly-negative. Hence, as (35) is always decreasing, there exists exactly one unique fixed point for the cSE of LAMA regardless of the noise variance  $N_0$ . Thus, LAMA achieves IO performance. The green dash-dotted and red dotted line in Fig. 4(a) show (35) for  $\beta < \beta_{\mathcal{O}}^{\min}$  with  $N_0 = 0$  and  $N_0 \simeq 0.15$ , respectively. In both cases, we see that the cSE of LAMA converges to the unique fixed point.

(ii)  $\beta_{\mathcal{O}}^{\min} \leq \beta \leq \beta_{\mathcal{O}}^{\max}$ : In this region, the cSE of LAMA converges to the unique, optimal fixed point if  $N_0 < N_0^{\min}(\beta)$  or if  $N_0 > N_0^{\max}(\beta)$  and consequently, LAMA achieves IO performance in both of these regimes. The green dash-dotted line, cyan dashed line, and magenta dotted line in Fig. 4(b) show (35) for  $\beta^* = (\beta_{\mathcal{O}}^{\min} + \beta_{\mathcal{O}}^{\max})/2$  with  $N_0 = 0$ ,  $N_0 > N_0^{\max}(\beta^*)$  and  $N_0 < N_0^{\min}(\beta^*)$ ,

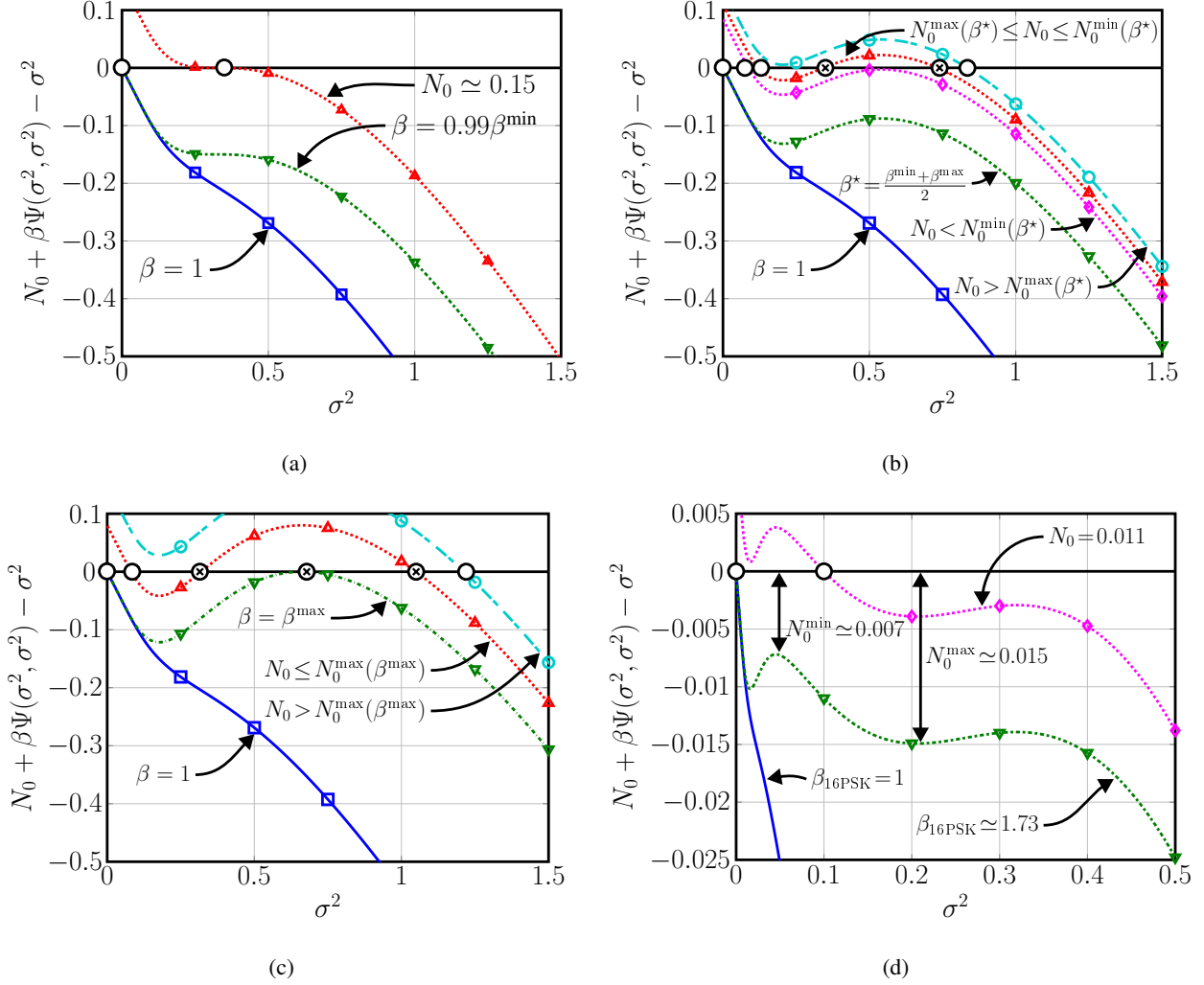


Fig. 4. Function (35) for three cases: (a)  $\beta < \beta_{\mathcal{O}}^{\min}$ , (b)  $\beta \in [\beta_{\mathcal{O}}^{\min}, \beta_{\mathcal{O}}^{\max}]$ , and (c)  $\beta > \beta_{\mathcal{O}}^{\max}$  for QPSK normalized to  $E_s = 1$ ; (d) is for 16-PSK and  $\beta = 1.73 \in [\beta_{\mathcal{O}}^{\min}, \beta_{\mathcal{O}}^{\max}]$ . Optimal fixed points are indicated by  $\circ$ ; suboptimal fixed points by  $\otimes$ . (a) For  $\beta < \beta_{\mathcal{O}}^{\min}$ , LAMA always converges to the unique, optimal fixed point, irrespective of the noise variance  $N_0$ . (b) For  $\beta \in [\beta_{\mathcal{O}}^{\min}, \beta_{\mathcal{O}}^{\max}]$ , we have two regimes for which LAMA converges to an optimal fixed point: (i)  $N_0 < N_0^{\min}(\beta)$  and (ii)  $N_0 > N_0^{\max}(\beta)$ . The situation  $\beta^* = \frac{\beta_{\mathcal{O}}^{\min} + \beta_{\mathcal{O}}^{\max}}{2}$  with (i)  $N_0 < N_0^{\min}(\beta^*)$  is shown with a purple dotted curve and (ii)  $N_0 > N_0^{\max}(\beta^*)$  is shown with a cyan dashed curve; we see that LAMA exhibits a single (and hence, optimal) fixed point. However, if  $N_0 \in [N_0^{\min}(\beta), N_0^{\max}(\beta)]$ , which is shown with a red dotted curve, the cSE of LAMA exhibits multiple fixed points and hence, LAMA is no longer IO. (c) For  $\beta > \beta_{\mathcal{O}}^{\max}$ , the cSE of LAMA converges to a suboptimal fixed point in the noiseless case  $N_0 = 0$ , which is shown in green. However, when  $N_0 > N_0^{\max}(\beta)$ , the cSE of LAMA converges to the optimal fixed point, which can be seen in the cyan dashed curve. If  $N_0 \leq N_0^{\min}(\beta)$ , then the cSE of LAMA, shown in red dotted curve, has multiple fixed points and thus, is no longer IO. (d) For 16-PSK and  $\beta = 1.73 \in [\beta_{\mathcal{O}}^{\min}, \beta_{\mathcal{O}}^{\max}]$ ,  $N_0^{\min}(\beta)$  and  $N_0^{\max}(\beta)$  is computed to be 0.007 and 0.015 respectively. For 16-PSK, there exists regions where  $N_0 \in [N_0^{\min}(\beta), N_0^{\max}(\beta)]$  and LAMA still achieves IO performance.

respectively. We note that for the three cases the fixed point is unique, labeled in Fig. 4(b) by a circle. The red, dotted line in Fig. 4(b) shows (35) with  $\beta^*$  for noise  $N_0 \in [N_0^{\min}(\beta^*), N_0^{\max}(\beta^*)]$ . In this case, however, we observe that the cSE of LAMA converges to the rightmost suboptimal fixed point labeled by the crossed circle  $\otimes$ . Hence, LAMA is able to achieve IO performance if  $N_0^{\min}(\beta) \leq N_0 \leq N_0^{\max}(\beta)$ .

(iii)  $\beta > \beta_{\mathcal{O}}^{\max}$ : In this region, the cSE of LAMA converges to the unique, optimal fixed point when  $N_0 > N_0^{\max}(\beta)$  and consequently, achieves IO performance. Unlike the previous case for  $\beta_{\mathcal{O}}^{\min} \leq \beta \leq \beta_{\mathcal{O}}^{\max}$ , for which LAMA has *two* regions of optimality,  $N_0 > N_0^{\max}(\beta)$  and  $N_0 < N_0^{\min}(\beta)$ , for  $\beta > \beta_{\mathcal{O}}^{\max}$ , LAMA has only one optimal region:  $N_0 > N_0^{\max}(\beta)$ . As  $\beta \rightarrow \beta_{\mathcal{O}}^{\max}$ , the low noise  $N_0 < N_0^{\min}(\beta)$  (or high *SNR*) region of optimality disappears because  $N_0^{\min}(\beta) \rightarrow 0$  as  $\beta \rightarrow \beta_{\mathcal{O}}^{\max}$  from (33). The green, dash-dotted line and red, dotted lines in Fig. 4(c) show (35) for  $\beta = \beta_{\mathcal{O}}^{\max}$  with  $N_0 = 0$  and  $0 < N_0 \leq N_0^{\max}(\beta)$ , respectively. We observe that the cSE of LAMA converges to the suboptimal fixed point when  $\beta = \beta_{\mathcal{O}}^{\max}$  even with  $N_0 = 0$ . The cyan, dashed line refers to  $\beta = \beta_{\mathcal{O}}^{\max}$  with  $N_0 > N_0^{\max}(\beta)$ . While the noiseless case enables the cSE of LAMA to converge to the suboptimal fixed point, we observe that for high noise (or equivalently low *SNR*), the cSE of LAMA is able to achieve IO performance. Therefore, if  $\beta > \beta_{\mathcal{O}}^{\max}$ , then LAMA achieves IO performance whenever the noise variance exceeds the maximum guaranteed noise variance  $N_0^{\max}(\beta)$ .

We also note that for some constellations, the cSE of LAMA may recover the optimal fixed point for  $\beta \in [\beta_{\mathcal{O}}^{\min}, \beta_{\mathcal{O}}^{\max}]$  in some noise variance intervals  $[N_0^{\min}(\beta), N_0^{\max}(\beta)]$ . An example case for  $\beta = 1.73$  with 16-PSK is shown in Fig. 4(d), where cSE of LAMA recovers the unique fixed-point with  $N_0 = 1.1 \cdot 10^{-2} \in [N_0^{\min}(\beta), N_0^{\max}(\beta)]$ . These intervals exist for some constellations because in addition to  $\sigma^2$  that result  $N_0^{\min}(\beta)$  and  $N_0^{\max}(\beta)$ , there are multiple values of  $\sigma^2$  that satisfy  $\frac{d}{d\sigma^2}g(\sigma^2, \beta, N_0, \mathcal{O}) = 0$ , where  $g(\sigma^2, \beta, N_0, \mathcal{O})$  is defined in (35). As a result, there exist intervals between  $N_0^{\min}(\beta)$  and  $N_0^{\max}(\beta)$  that the cSE of LAMA has one (optimal) fixed point. In such regions, LAMA enables IO performance. We finally note that the MRT  $\beta_{\mathcal{O}}^{\min}$  and ERT  $\beta_{\mathcal{O}}^{\max}$  do not depend on the signal variance  $\text{Var}_S[S]$ . In contrast, the critical noise levels  $N_0^{\min}(\beta)$  and  $N_0^{\max}(\beta)$  depend on  $\text{Var}_S[S]$ .

## F. Decomposing Complex-Valued Systems

We now analyze whether the cSE of LAMA with complex-valued constellations can equivalently be characterized by a real-valued SE with a real-valued constellation. We note that while the

loading factor limits were given in [76] and [16] respectively, these results were pertinent to BPSK with real-valued systems and no results were given for other constellations.

We note that the standard way of dealing with complex-valued systems is via the real-valued decomposition (see footnote 1). This approach, however, violates the independent assumption on the MIMO channel. Since LAMA operates directly on the complex plane, no transformation into the real-valued domain is required. Nevertheless, we now provide conditions for which the complex-valued problem can be exactly characterized by a corresponding real-valued problem. For our analysis, we require the following definition.

**Definition 10.** For all  $s \in \mathcal{O}$ , express  $s$  as  $s = a + ib$ , where  $a \in \text{Re}\{\mathcal{O}\}$ ,  $b \in \text{Im}\{\mathcal{O}\}$ . Then, the constellation  $\mathcal{O}$  is called separable if  $p(s) = p(a)p(b)$  holds for all  $s \in \mathcal{O}$  and  $\text{Re}\{\mathcal{O}\} = \text{Im}\{\mathcal{O}\}$ .

For example,  $M^2$ -QAM with equally likely symbols is separable. In contrast,  $M^2$ -PSK is not separable (except for QPSK) as the real and imaginary parts dependent. We now present a result that allows us to transform the complex-valued cSE equations in (12) and (13) into equivalent real-valued SE equations; the proof is given in Appendix L.

**Lemma 8.** Let the constellation  $\mathcal{O}$  be separable. Define  $S_{\text{R}} = \text{Re}\{S\}$  and denote the real-part of  $\mathcal{O}$  as  $\mathcal{O}^{\text{R}}$ . Define  $F^{\text{R}}$  and  $G^{\text{R}}$  as the message mean and variance function, respectively, with  $S_{\text{R}} \sim p(\text{Re}\{S\})$ . Also define the MSE function  $\Psi$  and the variance function  $\Phi$  for the real-valued prior  $S_{\text{R}}$  as:

$$\begin{aligned}\Psi^{\text{R}}(\sigma^2, \gamma^2) &= \mathbb{E}_{S_{\text{R}}, Z_{\text{R}}} \left[ \left( F^{\text{R}}(S_{\text{R}} + \sigma Z_{\text{R}}, \gamma^2) - S_{\text{R}} \right)^2 \right], \\ \Phi^{\text{R}}(\sigma^2, \gamma^2) &= \mathbb{E}_{S_{\text{R}}, Z_{\text{R}}} \left[ G^{\text{R}}(S_{\text{R}} + \sigma Z_{\text{R}}, \gamma^2) \right],\end{aligned}$$

where  $Z_{\text{R}} \sim \mathcal{N}(0, 1)$ . Then we have the following relation for  $\Psi$  and  $\Phi$  between the complex-valued constellation  $\mathcal{O}$  and the real-valued constellation  $\mathcal{O}^{\text{R}}$ :

$$\Psi(\sigma^2, \gamma^2) = 2\Psi^{\text{R}}\left(\frac{\sigma^2}{2}, \frac{\gamma^2}{2}\right), \quad \Phi(\sigma^2, \gamma^2) = 2\Phi^{\text{R}}\left(\frac{\sigma^2}{2}, \frac{\gamma^2}{2}\right).$$

Therefore, the cSE recursions in (12) and (13) are given by:

$$\sigma_t^2 = N_0 + \beta\Psi(\sigma_t^2, \gamma_t^2) = N_0 + 2\beta\Psi^{\text{R}}\left(\frac{\sigma_t^2}{2}, \frac{\gamma_t^2}{2}\right), \quad (36)$$

$$\gamma_t^2 = N_0^{\text{post}} + \beta\Phi(\sigma_t^2, \gamma_t^2) = N_0^{\text{post}} + 2\beta\Phi^{\text{R}}\left(\frac{\sigma_t^2}{2}, \frac{\gamma_t^2}{2}\right). \quad (37)$$

TABLE II

ERTs  $\beta_{\mathcal{O}}^{\max}$ , MRTs  $\beta_{\mathcal{O}}^{\min}$  AND THE CRITICAL NOISE LEVELS  $N_0^{\min}(\beta_{\mathcal{O}}^{\min})$  AND  $N_0^{\max}(\beta_{\mathcal{O}}^{\max})$  FOR LAMA WITH COMMON PSK, PAM, AND QAM CONSTELLATIONS

Constellation		$\beta_{\mathcal{O}}^{\min}$	$N_0^{\min}(\beta_{\mathcal{O}}^{\min})$	$\beta_{\mathcal{O}}^{\max}$	$N_0^{\max}(\beta_{\mathcal{O}}^{\max})$
$\mathbb{C}$ system	$\mathbb{R}$ system				
BPSK	–	2.951	$3.00 \cdot 10^{-1}$	4.171	$2.43 \cdot 10^{-1}$
QPSK	BPSK	1.475	$1.50 \cdot 10^{-1}$	2.086	$1.22 \cdot 10^{-1}$
16-QAM	4-PAM	0.983	$3.00 \cdot 10^{-2}$	1.363	$2.45 \cdot 10^{-2}$
64-QAM	8-PAM	0.842	$7.14 \cdot 10^{-3}$	1.157	$5.87 \cdot 10^{-3}$
256-QAM	16-PAM	0.786	$1.77 \cdot 10^{-3}$	1.075	$1.45 \cdot 10^{-3}$
8-PSK	–	1.458	$4.44 \cdot 10^{-2}$	1.804	$3.83 \cdot 10^{-2}$
16-PSK	–	1.473	$1.14 \cdot 10^{-2}$	1.801	$9.95 \cdot 10^{-3}$
64-PSK	–	1.474	$7.23 \cdot 10^{-4}$	1.801	$8.39 \cdot 10^{-3}$
256-PSK	–	1.474	$4.52 \cdot 10^{-5}$	1.801	$8.39 \cdot 10^{-3}$

We note that LAMA operates *simultaneously* on complex-valued signals by reducing  $\sigma_t^2$  each iteration in both real and imaginary parts independently; this can be seen by noting that since  $\mathcal{O}$  is separable,  $\Psi^{\mathbb{R}}$  is identical for both the real and imaginary parts of  $\mathcal{O}$ . In addition, Lemma 8 shows that if  $\mathcal{O}$  is separable, then the cSE can be transformed into a real-valued SE, hence validating the relation between the complex-valued constellation and the equivalent real-valued representation. This transformation implies that for certain constellations, the message mean  $F$  and variance function  $G$  can be computed (often more efficiently) in parallel for real and imaginary dimensions.

We note that in [3] Guo and Verdú used a real-valued decomposition and the replica method for analyzing the performance of complex-valued signals for separable constellations and concluded that the error performance for complex signals is exactly same as that of real-valued system with transmit energy halved. Lemma 8 supports this conclusion. Moreover, we emphasize that the cSE holds for *general* constellations, such as higher-order PSK constellations, and LAMA can be used for data detection in such cases.

### G. ERT, MRT, and Critical Noise Levels

The ERT, MRT, as well as the critical noise levels  $N_0^{\min}(\beta)$  and  $N_0^{\max}(\beta)$  for common constellations and for real-valued as well as complex-valued systems are summarized in Table II.

We assume equally likely priors with the constellation sets normalized to  $\text{Var}_S[S] = E_s = 1$ . We note that the calculations of ERT and MRT for the simplest case with BPSK involve computations of logistic-normal integrals for which no closed-form expressions are known [77] but approximations exist [77]–[79]. The results in Table II were obtained via numerical integration to compute the MSE function  $\Psi(\sigma^2, \sigma^2)$ .<sup>11</sup> Next Lemma shows that for real- and separable complex-valued constellations, the ERT and MRT are identical for real- and complex-valued systems, respectively; a short proof is given in Appendix M. For an example, BPSK for real-valued systems and QPSK for complex-valued systems have identical ERT and MRT of 1.475 and 2.086, respectively.

**Lemma 9.** *Fix a separable constellation  $\mathcal{O}$  and denote  $\beta_{\mathbb{C}}^{\min}$ ,  $\beta_{\mathbb{C}}^{\max}$  and  $\beta_{\mathbb{R}}^{\min}$ ,  $\beta_{\mathbb{R}}^{\max}$  as MRT and ERT of the complex and real-valued constellation, respectively. Also, denote the critical noise levels  $N_{0,\mathbb{C}}^{\max}(\beta)$ ,  $N_{0,\mathbb{C}}^{\min}(\beta)$ ,  $N_{0,\mathbb{R}}^{\max}(\beta)$ , and  $N_{0,\mathbb{R}}^{\min}(\beta)$  for the complex and real-valued constellation, respectively. Then,  $\beta_{\mathbb{C}}^{\min} = \beta_{\mathbb{R}}^{\min}$ ,  $\beta_{\mathbb{C}}^{\max} = \beta_{\mathbb{R}}^{\max}$ ,  $N_{0,\mathbb{C}}^{\max}(\beta) = 2N_{0,\mathbb{R}}^{\max}(\beta)$ , and  $N_{0,\mathbb{C}}^{\min}(\beta) = 2N_{0,\mathbb{R}}^{\min}(\beta)$ .*

Lemma 9 implies that optimality results for  $M^2$ -QAM in a complex system with equally likely transmit symbols (shown in Table II) are the same for a real-valued  $M$ -PAM system. Moreover, between BPSK and QPSK in a complex system, we observe that all the thresholds differ by a factor of 2, which is expected. As shown in the second row of Table II for QPSK with complex noise, or a real-valued BPSK system (with real noise) the ERT is  $\beta_{\text{QPSK}}^{\max} \approx 2.0855$ , which corresponds exactly to the maximum loading factor for the IO data detector established in [3], [16]. Moreover, the MRT for QPSK is given as  $\beta_{\text{QPSK}}^{\min} \approx 1.4752$  [16].<sup>12</sup> The critical noise values in Table II refer to complex constellations as the critical noise values can be easily computed for the real constellation by Lemma 9.

The MRTs for 16-QAM and 64-QAM indicate that small system ratios  $\beta < 1$  are necessary to guarantee that LAMA achieves IO performance. For instance, we require  $\beta \leq \beta_{64\text{-QAM}}^{\min} \approx 0.8424$ , i.e.  $M_T \leq 0.8424M_R$ , to ensure that LAMA solves (18) for 64-QAM. As  $\beta \rightarrow \beta_{64\text{-QAM}}^{\max} \approx 1.1573$ , LAMA is only optimal in settings in which the noise level is rather high, i.e., where  $N_0 > N_0^{\max}(\beta_{64\text{-QAM}}^{\max}) \approx 5.868 \cdot 10^{-3}$ , or, equivalently, when  $\text{SNR} < 22.9495$  dB. From Table II, we see that higher-order QAM or PSK constellations can be decoded optimally by LAMA in massive

<sup>11</sup>We used MATLAB's `integral` and `integral2` commands with `AbsTol = RelTol = 10-12`.

<sup>12</sup>Note that  $\beta_{\text{QPSK}}^{\min}$  Tanaka provided in [16] is 1.49, whereas we obtain a slightly more accurate value 1.4752.

MIMO as one typically assumes  $M_R \gg M_T$ . We also observe that as  $M$  increases for  $M$ -PSK,  $\beta_{\mathcal{O}}^{\min}$  and  $\beta_{\mathcal{O}}^{\max}$  approaches to 1.4741 and 1.8005, respectively.

## V. NUMERICAL RESULTS AND PRACTICAL CONSIDERATIONS

We now provide numerical results for LAMA, discuss practical implementation aspects, and highlight the pros and cons. In what follows, we use the average received SNR defined in (2).

### A. Achievable Rates and Error-Rate Performance

As detailed in Section III-C, the output of LAMA enables one to represent each transmit stream by a single-input single-output AWGN channel with a equal noise variance  $\sigma_t^2$  that can be computed via the cSE Theorem 1. Therefore, the performance of LAMA in the large-system limit can be characterized by analyzing a single AWGN channel.

Figures 5(a) and 5(b) show the achievable rate and symbol error rate for LAMA after 100 iterations for various system ratios  $\beta$ . While an infinite number of iterations would guarantee LAMA to converge to a fixed point solution, our results show that much fewer than 100 iterations are required for LAMA to converge; we will further discuss this aspect in Section V-B.

Fig. 5(a) shows the achievable rate of the decoupled AWGN channel per transmit stream for LAMA, for various system ratios  $\beta$ . For small values of  $\beta$ , e.g.  $\beta = 0.1$ , the achievable rate of LAMA approaches to that of an AWGN channel, which agrees with Lemma 4. We observe that the performance gap between LAMA and that of an AWGN channel increases with  $\beta$ . In particular, when  $\beta = \beta_{\text{QPSK}}^{\min}$ , we see a sudden transition in the achievable rate of LAMA to the achievable rate of an AWGN channel, which occurs approximately at 10 dB. This transition occurs exactly at the SNR regime for which the noise variance  $N_0$  becomes smaller than  $N_0^{\min}(\beta)$ , which was shown to ensure convergence of LAMA to the unique optimal fixed point (cf. Section IV-E). For  $\beta \rightarrow \beta_{\text{QPSK}}^{\max}$ , we see that the achievable rate does not converge to that of an interference-free AWGN channel, irrespective of the SNR regime; this agrees with the perfect recoverability result in the large-system limit shown in Theorem 5 for ERT  $\beta_{\text{QPSK}}^{\max}$ .

Fig. 5(b) shows the symbol error rate (SER) of LAMA. Similar to the achievable rate in Fig. 5(a), the SER for  $\beta = 0.1$  for LAMA in a MIMO system approaches that of an interference-free AWGN channel. For  $\beta > \beta^{\min}$ , we observe a waterfall behavior where the SER quickly drops and approaches that of an interference-free AWGN channel; this happens at exactly the point where the noise variance is smaller than the minimum critical noise  $N_0^{\min}(\beta_{\text{QPSK}}^{\min})$ . We note



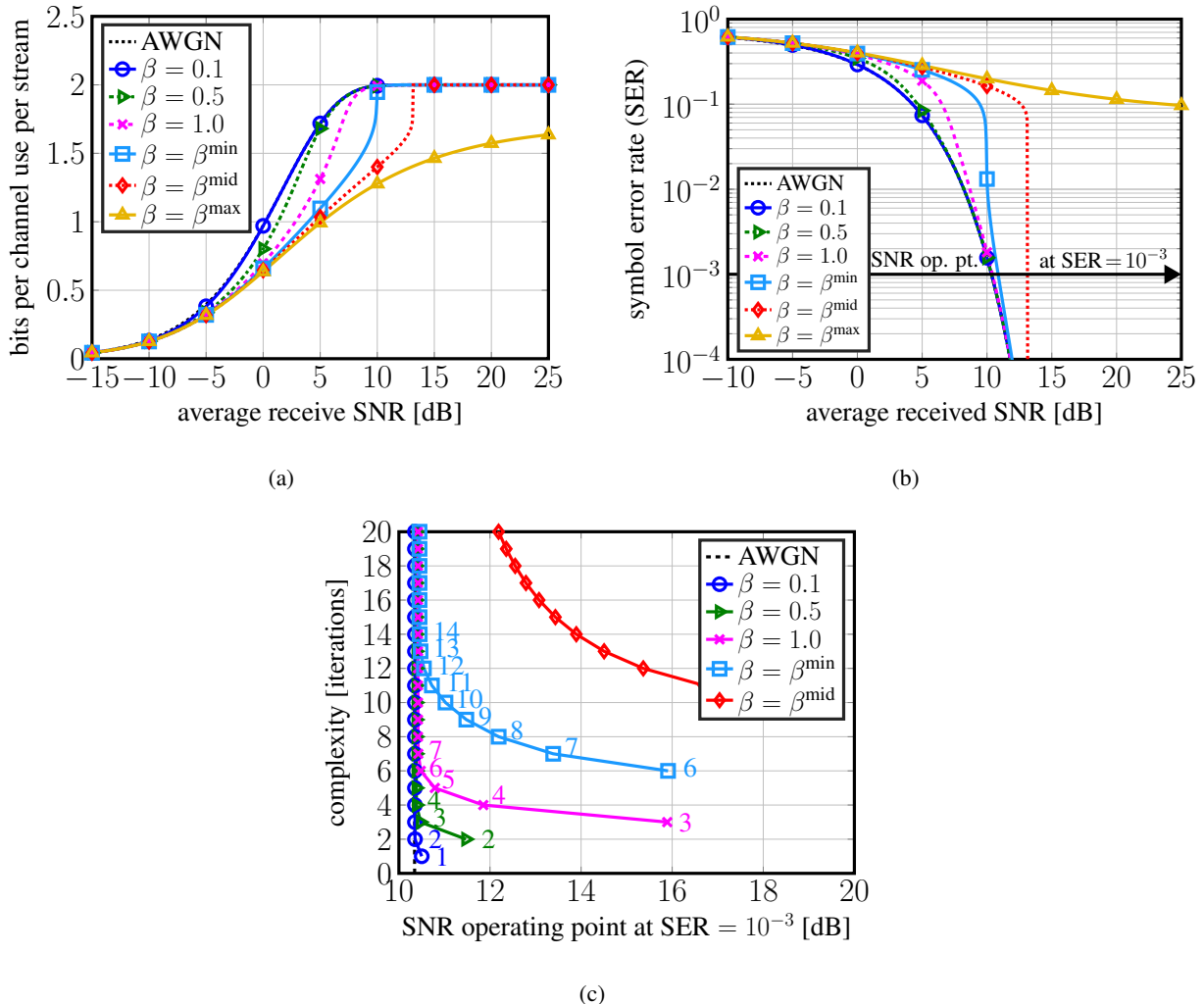


Fig. 5. (a) Achievable rate (in bits per channel use per stream), (b) symbol-error rate (SER), and (c) performance/complexity trade-offs of LAMA for  $\beta \in \{0.1, 0.5, \beta_{\text{QPSK}}^{\min}, \beta_{\text{QPSK}}^{\text{mid}}, \beta_{\text{QPSK}}^{\max}\}$ , where  $\beta_{\text{QPSK}}^{\text{mid}} = (\beta_{\text{QPSK}}^{\min} + \beta_{\text{QPSK}}^{\max})/2$ , and QPSK constellations. The sharp transitions in achievable rate and SER shown in (a) and (b) occur at  $\beta > \beta_{\text{QPSK}}^{\min}$  when the  $\text{SNR} = \beta \frac{E_s}{N_0}$  with  $N_0$  equaling the critical noise variance  $N_0^{\min}(\beta)$ . (c) The dashed lines refer to the SNR operating point for an AWGN channel at  $\text{SER} = 10^{-3}$  for each  $\beta$ . The atomic complexity of LAMA required to approach AWGN SNR increases with the system ratio  $M_T/M_R = \beta$ .

that this waterfall behavior is consistent with the SNR regime that caused an upwards jump in the achievable rate curve shown in Fig. 5(a). When  $\beta = \beta_{\text{QPSK}}^{\max}$ , we observe an SER floor at about 0.08; this is due to the fact that as  $\text{SNR} \rightarrow \infty$ , the cSE of LAMA always converges to a suboptimal fixed point shown in Fig. 4(c).

### B. Performance/Complexity Trade-off

While only an infinite number of LAMA iterations guarantee the cSE of LAMA in Theorem 1 to converge to a fixed-point of (31) and (32), one can terminate the algorithm early with the goal of reducing its complexity. A straightforward approach is to terminate Algorithm 2, if the parameter  $\tau^t$  does not improve from one iteration to the next, e.g., if  $\tau^t \leq \tau^{t+1}$  is met. Another approach is to terminate LAMA after a predefined number of  $I$  iterations. The latter approach not only enables a deterministic throughput (which is critical in hardware implementations), but also enables us to study a fundamental performance/complexity trade-off of LAMA.

Since the cSE analysis is only valid in the large system limit, common complexity measures, such as the number of additions and/or multiplications are not meaningful. Nevertheless, for a given system, we see from Algorithm 2 that the computational workload of LAMA per iteration remains constant. Hence, counting the maximum number of algorithm iterations provides a sensible way of measuring the complexity of LAMA<sup>13</sup>.

**Definition 11.** *The atomic complexity of LAMA is defined by the maximum number of algorithm iterations  $I$ .*

We now study the performance of LAMA depending on the atomic complexity  $I$ . Put simply, we investigate by how much one can approach the performance of LAMA with infinitely many iterations. We do so by first computing the output variance  $\sigma_I^2$  of the equivalent AWGN channel for a fixed complexity  $I$ , and then computing the associated SER.

We first discuss the convergence speed of LAMA to its fixed-point solution. The following result, with proof in Appendix N, reveals that if  $\beta < \beta_{\mathcal{O}}^{\min}$ , then LAMA not only has a unique fixed point solution, but also converges exponentially fast; this ensures that LAMA achieves near-IO performance with a small number of iterations.

**Lemma 10.** *Assume the initialization of LAMA as in Algorithm 2. If  $\beta < \beta_{\mathcal{O}}^{\min}$ , then regardless of the noise variance  $N_0$ , LAMA converges exponentially fast to its unique fixed-point solution  $\sigma_{\star}^2$ .*

Fig. 5(c) shows the required SNR to achieve SER of  $10^{-3}$  for every iteration of LAMA for various systems ratios  $\beta$  in the large-system limit. The colored dashed lines correspond to the

<sup>13</sup>In practice, one can multiply the atomic complexity with the number of arithmetic operations require per iteration; this enables one to obtain an accurate complexity measure that depends on the system configuration.

SNR required to achieve an SER of  $10^{-3}$  in an interference-free AWGN channel, which we call “AWGN SNR.” For  $\beta = 0.1$ ,  $\beta = 0.5$ , only three and five iterations are required for LAMA to closely approach the AWGN SNR. We observe that as  $\beta$  decreases, the number of iterations required to reach SNR of SER  $10^{-3}$  also decreases. This observation is in accordance with Lemma 4, where we demonstrated that in the extreme case where  $\beta \rightarrow 0$ , one iteration (matched filter detection) is sufficient to converge to the AWGN SNR. As  $\beta$  increases, we start to see the performance differences between LAMA and that of an interference-free AWGN channel. For  $\beta = \beta_{\text{QPSK}}^{\min}$ , the SNR operating point of LAMA closely approaches the AWGN SNR after 15 iterations at a small performance loss (about 0.1 dB), which is visible from the SER plot in Fig. 5(b). The differences between the SNR operating point of LAMA and AWGN SNR are more pronounced when  $\beta = (\beta_{\text{QPSK}}^{\min} + \beta_{\text{QPSK}}^{\max})/2$ , as the SNR operating point of LAMA converges to 13.5 dB after about 90 iterations, which is 0.6 dB higher than the AWGN SNR of 12.9 dB. For  $\beta = \beta_{\text{QPSK}}^{\max}$ , the complexity of LAMA is not shown as it floors to an SER of approximately 0.08 and hence, never achieves the target SER of  $10^{-3}$ .

### C. Performance in Finite-Dimensional Systems

Since the design of LAMA heavily relies on the large system limit, there are no optimality guarantees for finite-dimensional settings. For conventional, small-scale MIMO systems (with 8 antennas or less), the large-system assumption leads to a significant performance loss because (i) the statistics of  $\mathbf{z}^t = \hat{\mathbf{s}}^t + \mathbf{H}^H \mathbf{r}^t$  are not Gaussian and hence, (ii) the correct statistics of the Gaussian term  $\mathbf{z}^t$  cannot be tracked in the LAMA algorithm. The problem that arises in finite-dimensional systems becomes evident if we keep  $\beta = 1$  and increase  $\text{SNR} \rightarrow \infty$  for a small system. We see that LAMA exhibits in an SER floor (see Fig. 6(b) for a  $128 \times 128$  16-QAM system). We note that this SER floor lowers as the system’s dimension increases. The performance loss of AMP-based algorithms for small-sized systems has been investigated in [80], [81].

In order to mitigate LAMA’s performance loss in finite dimensional systems, one can use estimators as opposed to the original message variance function in (7) to estimate  $\sigma_t^2$  each iteration. For estimators in LAMA to work universally when the antenna configurations are *both* small and big, we need estimators of  $\sigma_{t+1}^2$ , which we will denote as  $\hat{\sigma}_{t+1}^2$ , that not only lower the error floor at high SNR in small antenna systems, but also converges to the true effective noise variance  $\sigma_{t+1}^2$  in large antenna systems.

In [34], a series of estimators have been proposed for AMP in the context of sparse recovery. We adopt the same approach for LAMA for the case  $N_0^{\text{post}} = N_0$ , where instead of computing the average of the exact message variance function as (11), we estimate the variance of the Gaussian estimate  $\mathbf{z}^t = \hat{\mathbf{s}}^t + \mathbf{H}^H \mathbf{r}^t$  by:

$$\hat{\sigma}_{t+1}^2 = \frac{1}{M_R} \|\mathbf{r}^t\|_2^2. \quad (38)$$

Fig. 6(b) shows the performance of (38) for LAMA in an  $128 \times 128$  system with 16-QAM. We observe a decrease in the SER floor in high SNR regime compared to the original LAMA without the estimator with no performance loss in the low SNR regime.

#### D. Extension to General Channel Matrices $\mathbf{H}$

It is important to note that one of the limiting assumptions underlying AMP (and hence, for LAMA) is that the entries of the channel matrix  $\mathbf{H}$  are i.i.d. zero-mean Gaussian or complex Gaussian with variance  $1/M_R$  for AMP and complex-valued AMP respectively. In practical systems, however, the BS antennas may exhibit correlation and uneven power profiles, especially in multi-user scenarios, which makes LAMA less robust in these scenarios. To address these limitations, Rangan [38] has developed Generalized AMP (GAMP), which extends AMP to arbitrary input and output noise distributions for real-valued systems, and can operate in channels with different power profiles. We note that in the large system limit with  $\mathbf{H}$  distributed according to (A2) with Gaussian noise, GAMP and AMP are equivalent. In addition, a modified GAMP that uses damping technique was proposed in [82] to cope with non-zero mean, low-rank channels. The damping technique slows certain algorithmic parameter updates, but does so at the cost of increased iterations of the algorithm. Vila and Schniter furthermore included expectation-maximization into GAMP in [41], [50], which further improves the performance of AMP-based methods in finite-dimensional systems. Recently, reference [40] introduced vector AMP, which further generalizes GAMP to arbitrary matrices.

Generalized AMP has been used for practical MIMO-OFDM systems [53] with variations introduced in [41], [50], [52] to increase the detection performance for a finite-dimensional system. Reference [53] primarily focused on simulations, whereas our paper concentrates on theoretical analysis in the large-system limit via the state-evolution framework.

### E. Simulation Results

Figures 6(a) and 6(b) show simulation results for large MIMO systems with 16-QAM. We fix the number of BS antennas to 128 and the number of user antennas to 64 and 128. We compare the performance of LAMA to unbiased linear MMSE detection, another message-passing-based receiver, i.e., channel hardening-exploiting message passing (CHEMP) [66]<sup>14</sup>, and IO data detection bound obtained by the cSE in the large-system limit.

For the  $128 \times 64$  system in Fig. 6(a), LAMA performs very close to the IO bound with only 8 iterations. We note that CHEMP [66] with 8 iterations performs worse than the linear MMSE detection, but approaches the performance of LAMA at 15 iterations. Note that in the large-system limit for a system-ratio of  $\beta = 64/128$ ,  $\beta < \beta_{16\text{QAM}}^{\min}$ , so LAMA achieves IO data detection performance for any noise variance  $N_0$ .

For the  $128 \times 128$  system in Fig. 6(b), LAMA with the estimator in (38) exhibits a floor at around  $10^{-2}$  SER. We note that LAMA with the estimator reduces the error floor while maintaining the performance at low SNR. Because of the flooring behavior of LAMA in finite dimensions, it performs worse than linear MMSE at high SNR (above 35 dB for this case). LAMA with 20 iterations outperforms CHEMP at the same number of iterations; CHEMP floors at an SER of  $10^{-1}$  even after 100 iterations. In the  $128 \times 128$  setting, we note that  $\beta = 1$  is larger than the ERT,  $\beta_{16\text{QAM}}^{\min} \approx 0.9830$ , from Table II, so LAMA has two regions of optimality (cf. Table I for the regions) with  $N_0^{\min}(\beta) \approx 0.03$ , or SNR around 15 dB. Note that this SNR happens where the sharp “waterfall” appears in the IO bound in Fig. 6(b). We stress that for  $\beta = 1$  and  $M_T \rightarrow \infty$ , the SER of LAMA will converge to that of the IO bound by cSE.

## VI. LAMA AND PRIOR ART

We now review existing results that are relevant for LAMA and our analysis in Section IV-E.

### A. BPSK signaling in Randomly Spread CDMA systems

We show that LAMA for BPSK constellation in randomly spread CDMA systems coincides exactly to the detection algorithm put forth in [17] and the cSE of LAMA without noise variance mismatch is equivalent to that given by IO data detection bound derived from the replica method by

<sup>14</sup> We note that CHEMP has no theoretical performance guarantees and was primarily developed for massive MIMO, i.e.,  $M_R \gg M_T$  or small  $\beta$ .

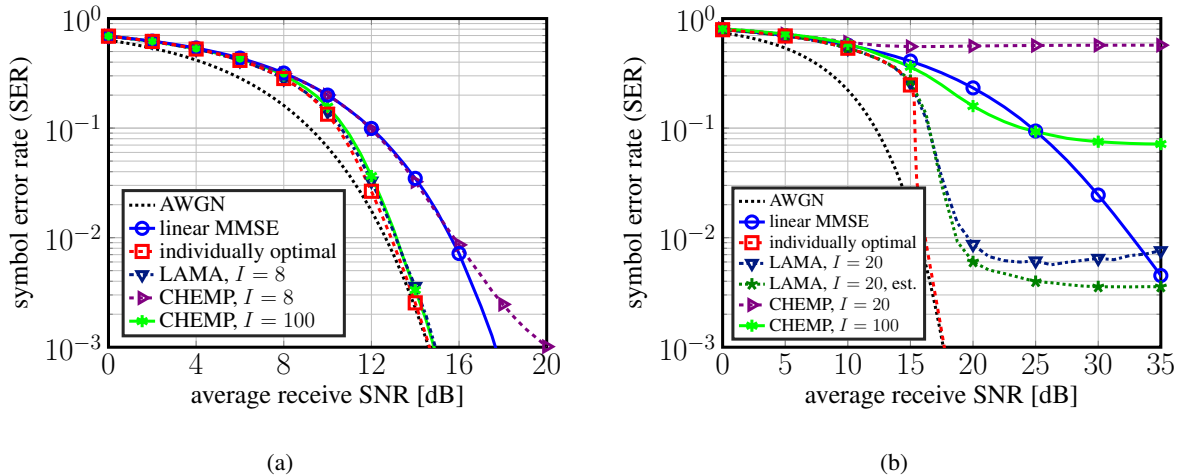


Fig. 6. Symbol error rate (SER) performance of LAMA for finite-dimensional systems with 16-QAM. (a) SER for a  $128 \times 64$  system, compared to linear MMSE detection and CHEMP [66]. (b) SER for a  $128 \times 128$  system, with the estimator in (38) for LAMA to mitigate the performance loss occurring from finite dimensions.

Tanaka in [16]. Consider a real-valued randomly-spread CDMA system with equally likely BPSK symbols  $\mathcal{O} = \{-1, +1\}$  and the entries of the channel matrix  $\mathbf{H}$  are distributed  $\mathcal{N}(0, 1/M_R)$ . In this case, (20) and (21) are given by

$$F(\hat{s}_\ell, \tau) = \tanh\left(\frac{1}{\tau} \hat{s}_\ell\right), \quad G(\hat{s}_\ell, \tau) = 1 - \tanh^2\left(\frac{1}{\tau} \hat{s}_\ell\right).$$

and thus, LAMA corresponds to the following recursion:

$$\begin{aligned} \hat{\mathbf{s}}^{t+1} &= \tanh\left(\frac{\hat{\mathbf{s}}^t + \mathbf{H}^T \mathbf{r}^t}{N_0(1 + \tau^t)}\right) \\ \tau^{t+1} &= \frac{\beta}{N_0} \left\langle 1 - \tanh^2\left(\frac{\hat{\mathbf{s}}^t + \mathbf{H}^T \mathbf{r}^t}{N_0(1 + \tau^t)}\right) \right\rangle \\ \mathbf{r}^{t+1} &= \mathbf{y} - \mathbf{H} \hat{\mathbf{s}}^{t+1} + \frac{\tau^{t+1}}{1 + \tau^t} \mathbf{r}^t, \end{aligned}$$

with the SE recursion from Theorem 1 given by

$$\sigma_{t+1}^2 = N_0 + \beta \mathbb{E}_{S,Z} \left[ \left( \tanh\left(\frac{S + \sigma_t Z}{\sigma_t^2}\right) - S \right)^2 \right], \quad (39)$$

where for a fixed  $\beta$  and  $N_0$ , the fixed point equation is

$$\sigma^2 = N_0 + \beta \int_{\mathbb{R}} \left[ 1 - \tanh\left(\frac{1 + \sigma z}{\sigma^2}\right) \right] \frac{1}{\sqrt{2\pi}} \exp\left(-\frac{z^2}{2}\right) dz. \quad (40)$$

We note that the fixed point equation in (40) coincides exactly to Tanaka's fixed point equation in [16] and the optimal multiuser efficiency in [3] derived using the replica method. Moreover,

LAMA coincides exactly to the method developed by Kabashima in 2003 for randomly-spread CDMA with BPSK signaling [17]. Kabashima showed that the algorithm is consistent with the state evolution predictions obtained through numerical simulations. Kabashima's algorithm in [17] was given for BPSK in real-valued systems only; in contrast, LAMA is suitable for general constellations and complex-valued systems, and can be analyzed in the large-system limit.

In Section IV-G, we noted that the ERT of a BPSK system for LAMA is computed to be approximately 2.0855, which coincides exactly with Tanaka's recovery threshold in [16], which was computed using the replica method. While we characterized the state of having multiple fixed point solutions by our definitions of MRT and ERT, Tanaka analogized the state of having multiple fixed points as having coexistence of phases in physical systems. In this context, the MRT  $\beta_{\text{BPSK}}^{\min}$  and ERT  $\beta_{\text{BPSK}}^{\max}$  corresponds to the boundary in which the instability of the phrases occur, and the boundary where the replica-symmetry solution becomes unstable, breaking the replica-symmetry assumptions [16]. Although an analytical expression of the ERT has been given in [16], an exact characterization of the MRT was not included. Note that our LAMA results generalize Tanaka's results to arbitrary constellations and provide a practical algorithm.

### B. Recovery of Antipodal Solutions via Convex Optimization

Recall that from Table II, that a system ratio  $\beta$  smaller than 2.0855 is able to perfectly recover a BPSK vector in absence of noise. In this scenario, LAMA is able to determine the unique solution to  $\mathbf{y} = \mathbf{H}\mathbf{s}_0$  with  $\mathbf{s}_0 \in \{-1, +1\}^{M_T}$  if  $\mathbf{H}$  is distributed (A2), and  $\beta = M_T/M_R$  is fixed with  $M_T \rightarrow \infty$ . A similar scenario was studied in [74], [83], where the authors have provided necessary and sufficient conditions for the recovery of antipodal solutions from  $\mathbf{y} = \mathbf{H}\mathbf{s}_0$ . In [74], Donoho and Tanner showed that in the large system limit,  $\beta < 2$  guarantees the recoverability of the unique signal  $\mathbf{s}_0 \in \{-1, +1\}^{M_T}$ . The same threshold was recovered in [83], by solving the following convex optimization problem [84]:

$$(\mathbf{P}_\infty) \quad \underset{\tilde{\mathbf{s}} \in \mathbb{R}^{M_T}}{\text{minimize}} \quad \|\tilde{\mathbf{s}}\|_\infty \quad \text{subject to } \mathbf{y} = \mathbf{H}\tilde{\mathbf{s}}.$$

In particular, the solution  $\hat{\mathbf{s}}$  to  $(\mathbf{P}_\infty)$  corresponds to the antipodal vector  $\{-\alpha, +\alpha\}$  for a given  $\alpha > 0$  if  $\beta < 2$  with high probability [83]. It is interesting to see that  $(\mathbf{P}_\infty)$  does not exploit magnitude information (i.e.  $\alpha = 1$ ), whereas LAMA requires this information. Quite surprisingly, the lack of this prior information only results in a slight improvement in terms of the system

ratio  $\beta$  that enables perfect recovery from 2 to 2.0855. The error-rate performance of  $\hat{\mathbf{s}}$  to  $(\mathbf{P}_\infty)$  for was recently investigated in [85]–[87]; LAMA-based results were studied in [59].

## VII. CONCLUSIONS

In this paper, we have developed the complex Bayesian approximate message passing (cB-AMP) framework with a possible mismatch in the postulated noise variance; cB-AMP with appropriate priors enables a derivation of the LAMA data detector. In the large-system limit, we have shown that LAMA decouples large MIMO systems into parallel AWGN channels with identical noise variance across all transmit streams every iteration. Furthermore, cSE has been used to analyze the exact noise variance of the decoupled AWGN channel.

We have derived the specific conditions for which LAMA achieves IO performance. Based on the system ratio  $\beta$ , there exist three optimality regimes for LAMA, where  $\beta \leq \beta_{\mathcal{O}}^{\min}$ ,  $\beta \in (\beta_{\mathcal{O}}^{\min}, \beta_{\mathcal{O}}^{\max})$ , and  $\beta \geq \beta_{\mathcal{O}}^{\max}$  where the MRT  $\beta_{\mathcal{O}}^{\min}$  and ERT  $\beta_{\mathcal{O}}^{\max}$  can be computed numerically for LAMA. We have shown both asymptotic and finite-dimensional performance of LAMA through analytical predictions and numerical simulations, which confirm our theoretical results. In addition, we have characterized the convergence behavior of LAMA for system ratios smaller than the ERT. For small system ratios  $\beta$ , we have shown that LAMA exhibits similar achievable rate and error-rate performance to that of an AWGN channel for a low number of iterations, which makes LAMA an excellent candidate for data detection in massive MIMO systems.

There are numerous avenues for further work. A performance analysis of LAMA with noise variance mismatch and a theoretical study in the finite dimensional setting as in [88] are open problems. Moreover, theoretical analysis of LAMA and (AMP-based) methods for non-i.i.d. channel matrices could lead to a more robust algorithms that can operate more effectively on practical, real-world channel matrices. Investigating the performance of LAMA in the presence of mismatched priors, as in [59], [89], may lead to hardware-friendly data detection algorithms. A hardware implementation of LAMA would demonstrate the real-world efficacy of our algorithm.

## ACKNOWLEDGMENTS

The work of C. Jeon, R. Ghods, and C. Studer was supported in part by Xilinx Inc., and by the US National Science Foundation (NSF) under grants ECCS-1408006, CCF-1535897, CAREER CCF-1652065, CNS-1717559, and EECS-1824379.



## APPENDIX A

[30, LEM. 5.56]

For completeness, we include [30, Lem. 5.56] and its proof for complex-valued MIMO systems. We will use Lemma 11 to derive the cB-AMP algorithm in Appendix B.

**Lemma 11.** *Let  $\hat{s}_{\ell \rightarrow k}^t$  and  $N_0^{\text{post}} \tau_{\ell \rightarrow k}^t$  be the mean and variance of the distribution  $\nu_{\ell \rightarrow k}^t$  in (42), respectively. Suppose at iteration  $t$ , the messages are set to  $\hat{\nu}_{k \rightarrow \ell}^t(s_\ell) = \hat{\phi}_{k \rightarrow \ell}^t(s_\ell)$ , where  $\hat{\phi}_{k \rightarrow \ell}^t(s_\ell)$  is defined by*

$$\hat{\phi}_{k \rightarrow \ell}^t(s_\ell) \triangleq \frac{|H_{k,\ell}|^2}{\pi N_0^{\text{post}}(1 + \tau_{k \rightarrow \ell}^t)} \exp\left(-\frac{|H_{k,\ell}s_\ell - r_{k \rightarrow \ell}^t|^2}{N_0^{\text{post}}(1 + \tau_{k \rightarrow \ell}^t)}\right), \quad (41)$$

and  $\tau_{k \rightarrow \ell}^t = \tau^t$ , where the residual and variance terms are given by

$$r_{k \rightarrow \ell}^t \triangleq y_k - \sum_{b \neq \ell} H_{k,b} \hat{s}_{b \rightarrow k}, \quad \tau_{k \rightarrow \ell}^t \triangleq \sum_{b \neq \ell} |H_{k,b}|^2 \tau_{b \rightarrow k}^t.$$

Then, at the next iteration  $t + 1$ , the mean and the variance of the message  $\nu_{\ell \rightarrow k}^{t+1}$  are given by

$$\begin{aligned} \hat{s}_{\ell \rightarrow k}^{t+1} &= \text{F}\left(\sum_{a \neq k} H_{a,\ell}^* r_{a \rightarrow \ell}^t, N_0^{\text{post}}(1 + \tau^t)\right), \\ \tau_{\ell \rightarrow k}^{t+1} &= \frac{1}{N_0^{\text{post}}} \text{G}\left(\sum_{a \neq k} H_{a,\ell}^* r_{a \rightarrow \ell}^t, N_0^{\text{post}}(1 + \tau^t)\right), \end{aligned}$$

*Proof.* Suppose at iteration  $t$ , the messages from factor nodes to the variable nodes are set to be  $\hat{\nu}_{k \rightarrow \ell}^t = \hat{\phi}_{k \rightarrow \ell}^t$ . Then,

$$\begin{aligned} \nu_{\ell \rightarrow k}^{t+1} &= \prod_{a \neq k} \hat{\phi}_{a \rightarrow \ell}^t(s_\ell) \\ &= \exp\left(-\frac{\sum_{a \neq k} |H_{a,\ell}s_\ell - r_{a \rightarrow \ell}^t|^2}{N_0^{\text{post}}(1 + \tau_{k \rightarrow \ell}^t)}\right) p(s_\ell) \\ &= \frac{1}{Z} \exp\left(-\frac{|s_\ell|^2 - 2 \sum_{a \neq k} \text{Re}\{s_\ell^* H_{a,\ell}^* r_{a \rightarrow \ell}^t\}}{N_0^{\text{post}}(1 + \tau_{k \rightarrow \ell}^t)}\right) \\ &\quad \cdot \exp\left(\frac{|s_\ell|^2}{M_{\text{R}} N_0^{\text{post}}(1 + \tau_{k \rightarrow \ell}^t)}\right) p(s_\ell) \\ &= \phi_{\ell \rightarrow k}^{t+1}(s_\ell) \{1 + O(|s_\ell|^2 / M_{\text{R}})\}, \end{aligned}$$

where  $Z$  is a normalization constant that ensures  $\nu_{\ell \rightarrow k}^{t+1}$  is a probability density function. Here, we defined  $\phi_{\ell \rightarrow k}^{t+1}$  as

$$\phi_{\ell \rightarrow k}^{t+1}(s_\ell) = f\left(s_\ell \left| \sum_{a \neq k} H_{a,\ell}^* r_{a \rightarrow \ell}^t, N_0^{\text{post}}(1 + \tau^t)\right.\right),$$

where  $f(s_\ell | \hat{s}_\ell, \tau)$  is defined as the probability distribution in (5) and  $\tau_{k \rightarrow \ell}^t = \tau^t$ . By definition, the mean  $F$  and variance  $G$  of  $\nu_{\ell \rightarrow k}^{t+1}$  is given as mean and variance of the conditional probability distribution defined in (5):

$$\begin{aligned}\hat{s}_{\ell \rightarrow k}^{t+1} &= F \left( \sum_{a \neq k} H_{a,\ell}^* r_{a \rightarrow \ell}^t, N_0^{\text{post}}(1 + \tau^t) \right), \\ \tau_{\ell \rightarrow k}^{t+1} &= \frac{1}{N_0^{\text{post}}} G \left( \sum_{a \neq k} H_{a,\ell}^* r_{a \rightarrow \ell}^t, N_0^{\text{post}}(1 + \tau^t) \right).\end{aligned}$$

□

## APPENDIX B

### DERIVATION OF ALGORITHM 1

We start by considering a factor graph  $G = (V, F, E)$  with variable nodes  $V = \{1, \dots, M_T\}$ , factor nodes  $F = \{1, \dots, M_R\}$ , and edges  $E = V \times F = \{(\ell, k) : \ell \in V, k \in F\}$ . The sum-product message equations for (4) at every iteration  $t$  are given by [55],

$$\nu_{\ell \rightarrow k}^t(s_\ell) = \prod_{a \neq k} \hat{\nu}_{a \rightarrow \ell}^{t-1}(s_\ell) p(s_\ell), \quad (42)$$

$$\hat{\nu}_{k \rightarrow \ell}^t(s_\ell) = \int_{\mathbb{C}} p(y_k | \mathbf{s}, \mathbf{h}_k^r) \prod_{b \neq \ell} \nu_{b \rightarrow k}^t(s_b) dy_k, \quad (43)$$

where  $\nu_{\ell \rightarrow k}^t(s_\ell)$  and  $\hat{\nu}_{k \rightarrow \ell}^t(s_\ell)$  are probability density functions.

Now, with Lemma 11 we can simplify the sum-product algorithm shown in (42) and (43). We first expand the messages  $\hat{s}_{\ell \rightarrow k}^{t+1}$  and  $r_{k \rightarrow \ell}^{t+1}$  into two parts (i) constant messages  $\hat{s}_\ell^{t+1}$  and  $r_k^{t+1}$  which are independent of the edge  $(\ell, k)$  and (ii) perturbed messages  $\Delta \hat{s}_{\ell \rightarrow k}^{t+1}$ ,  $\Delta r_{k \rightarrow \ell}^{t+1}$  that depend on the edge. As done in [37, Eq. 5], we assume  $\Delta \hat{s}_{\ell \rightarrow k}^{t+1}, \Delta r_{k \rightarrow \ell}^{t+1} = O(1/\sqrt{M_T})$  such that

$$\hat{s}_{\ell \rightarrow k}^{t+1} \triangleq \hat{s}_\ell^{t+1} + \Delta \hat{s}_{\ell \rightarrow k}^{t+1} + O(1/M_T), \quad (44)$$

$$r_{k \rightarrow \ell}^{t+1} \triangleq r_k^{t+1} + \Delta r_{k \rightarrow \ell}^{t+1} + O(1/M_T). \quad (45)$$

We then replace the complex-valued soft-thresholding function  $\eta(\cdot)$  by the conditional mean  $F(\cdot)$  as in [37, Prop. II.1], and use the decomposition in (44) and (45) to obtain

$$\begin{aligned}\hat{s}_\ell^{t+1} &= F \left( \hat{s}_\ell^t + \sum_{a=1}^{M_R} H_{a,\ell}^* r_a^t, N_0^{\text{post}}(1 + \tau^t) \right) \\ r_k^{t+1} &= y_k - \sum_{b=1}^{M_T} H_{k,b} \hat{s}_b^{t+1}\end{aligned} \quad (46)$$

$$\begin{aligned}
& + \sum_{b=1}^{M_T} H_{k,b} \left( \partial_1 \mathbf{F}^{\mathbf{R}} \left( \hat{s}_b^t + \sum_{a=1}^{M_R} H_{a,b}^* r_a^t \right) \right) \text{Re} \{ H_{k,b}^* r_k^t \} \\
& + \sum_{b=1}^{M_T} H_{k,b} \left( \partial_2 \mathbf{F}^{\mathbf{R}} \left( \hat{s}_b^t + \sum_{a=1}^{M_R} H_{a,b}^* r_a^t \right) \right) \text{Im} \{ H_{k,b}^* r_k^t \} \\
& + i \sum_{b=1}^{M_T} H_{k,b} \left( \partial_1 \mathbf{F}^{\mathbf{I}} \left( \hat{s}_b^t + \sum_{a=1}^{M_R} H_{a,b}^* r_a^t \right) \right) \text{Re} \{ H_{k,b}^* r_k^t \} \\
& + i \sum_{b=1}^{M_T} H_{k,b} \left( \partial_2 \mathbf{F}^{\mathbf{I}} \left( \hat{s}_b^t + \sum_{a=1}^{M_R} H_{a,b}^* r_a^t \right) \right) \text{Im} \{ H_{k,b}^* r_k^t \}, \tag{47}
\end{aligned}$$

with

$$\begin{aligned}
\partial_1 \mathbf{F}^{\mathbf{R}} & \triangleq \frac{\partial \text{Re} \{ \mathbf{F}(x + iy, \tau) \}}{\partial x}, & \partial_2 \mathbf{F}^{\mathbf{R}} & \triangleq \frac{\partial \text{Re} \{ \mathbf{F}(x + iy, \tau) \}}{\partial y}, \\
\partial_1 \mathbf{F}^{\mathbf{I}} & \triangleq \frac{\partial \text{Im} \{ \mathbf{F}(x + iy, \tau) \}}{\partial x}, & \partial_2 \mathbf{F}^{\mathbf{I}} & \triangleq \frac{\partial \text{Im} \{ \mathbf{F}(x + iy, \tau) \}}{\partial y}.
\end{aligned}$$

The final step to arrive at the cB-AMP algorithm is to compute the message-variance update equation and simplifying (47) by the fact that  $\mathbf{H}$  satisfies (A1). We note that the message-variance update equation was not provided in [37] and hence, we include it for completeness. The variance update equation is computed by

$$\begin{aligned}
\tau^{t+1} & = \sum_{b=1}^{M_T} |H_{k,b}|^2 \tau_{b \rightarrow k}^{t+1} \\
& = \sum_{b=1}^{M_T} \frac{1}{N_0^{\text{post}} M_R} \mathbf{G} \left( \hat{s}_b^t + \sum_{a=1}^{M_R} H_{a,b}^* r_a^t, N_0^{\text{post}} (1 + \tau^t) \right). \tag{48}
\end{aligned}$$

Since the columns of  $\mathbf{H}$  have unit norm with pairwise independence by (A1), each term in (47) can be simplified in the large system limit as follows:

$$\begin{aligned}
\sum_{b=1}^{M_T} H_{k,b} \partial_1 \mathbf{F}^{\mathbf{R}} \text{Re} \{ H_{k,b}^* r_k^t \} & = \frac{\beta}{2} r_k^t \langle \partial_1 \mathbf{F}^{\mathbf{R}} \rangle, \\
\sum_{b=1}^{M_T} H_{k,b} \partial_2 \mathbf{F}^{\mathbf{R}} \text{Im} \{ H_{k,b}^* r_k^t \} & = \frac{\beta}{2i} r_k^t \langle \partial_2 \mathbf{F}^{\mathbf{R}} \rangle, \\
i \sum_{b=1}^{M_T} H_{k,b} \partial_1 \mathbf{F}^{\mathbf{I}} \text{Re} \{ H_{k,b}^* r_k^t \} & = \frac{\beta i}{2} r_k^t \langle \partial_1 \mathbf{F}^{\mathbf{I}} \rangle, \\
i \sum_{b=1}^{M_T} H_{k,b} \partial_2 \mathbf{F}^{\mathbf{I}} \text{Im} \{ H_{k,b}^* r_k^t \} & = \frac{\beta}{2} r_k^t \langle \partial_2 \mathbf{F}^{\mathbf{I}} \rangle,
\end{aligned}$$

By using the Hadamard product, we arrive at Algorithm 1.

## APPENDIX C

## PROOF OF LEMMA 1

We use the facts that  $\partial_2 F^R$ ,  $\partial_1 F^I$ , and  $\partial_2 F^I$  are all zero for real-valued systems. Moreover, since the  $\ell_2$ -norm of each column of  $\mathbf{H}$  is one according to (A1), the update (47) simplifies to

$$\begin{aligned} r_k^{t+1} - (y_k - \mathbf{h}_k^r \hat{\mathbf{s}}^{t+1}) &= r_k^t \sum_{b=1}^{M_T} H_{k,b}^2 F' \left( \hat{s}_b^t + \sum_{a=1}^{M_R} H_{a,b} r_a^t \right) \\ &= \beta r_k^t \langle F'(\hat{\mathbf{s}}^t + \mathbf{H}^T \mathbf{r}^t) \rangle, \end{aligned} \quad (49)$$

where  $F'$  is the derivative of the mean function  $F(\hat{s}_\ell, \tau)$  taken with respect to  $\hat{s}_\ell$ . The final comparison of (49) with [30, Eq. 5.74] reveals equivalence of real-valued cB-AMP and B-AMP.

## APPENDIX D

## INTUITIVE DERIVATION OF THEOREM 1

We present a non-rigorous derivation of Theorem 1 for complex-valued systems; a rigorous proof can be found in [29]. Assume that the MIMO channel  $\mathbf{H}(t)$  changes each iteration  $t$ , where the elements are distributed  $\mathcal{CN}(0, 1/M_R)$ . In addition, let  $F(z, \tau)$  and  $G(z, \tau)$  are functions defined in (6) and (7) according to the mean and variance of the distribution in (5), respectively. Let  $\mathbf{y}^t = \mathbf{H}(t)\mathbf{s}_0 + \mathbf{n}$  where the entries of  $\mathbf{n}$  are circularly symmetric complex Gaussian with variance  $N_0$ . Assuming that we fix the postulated noise variance to  $N_0^{\text{post}}$ , then, in each iteration, the recursion is defined as:

$$\mathbf{r}^t = \mathbf{y}^t - \mathbf{H}\hat{\mathbf{s}}^t, \quad (50)$$

$$\hat{\mathbf{s}}^{t+1} = F(\hat{\mathbf{s}}^t + \mathbf{H}^H(t)\mathbf{r}^t, N_0^{\text{post}}(1 + \tau^t)), \quad (51)$$

$$\tau^{t+1} = \frac{\beta}{N_0^{\text{post}}} \langle G(\hat{\mathbf{s}}^t + \mathbf{H}^H(t)\mathbf{r}^t, N_0^{\text{post}}(1 + \tau^t)) \rangle. \quad (52)$$

By substituting  $\mathbf{r}^t$  in (50) into  $\hat{\mathbf{s}}^t + \mathbf{H}^H(t)\mathbf{r}^t$ , we have that

$$\begin{aligned} \hat{\mathbf{s}}^t + \mathbf{H}^H(t)\mathbf{r}^t &= \mathbf{H}^H(t)\mathbf{y}^t + (\mathbf{I}_{M_T} - \mathbf{H}^H(t)\mathbf{H}(t))\hat{\mathbf{s}}^t \\ &= \mathbf{s}_0 + \mathbf{H}^H(t)\mathbf{n} + (\mathbf{I}_{M_T} - \mathbf{H}^H(t)\mathbf{H}(t))(\hat{\mathbf{s}}^t - \mathbf{s}_0). \end{aligned} \quad (53)$$

The central limit theorem shows that each diagonal and non-diagonal entry in  $\mathbf{I}_{M_T} - \mathbf{H}^H(t)\mathbf{H}(t)$  is distributed  $\mathcal{N}(0, 1/M_R)$  and  $\mathcal{CN}(0, 1/M_R)$  respectively, with pairwise independent entries. Also, for each  $\ell$ th entry in  $(\mathbf{I}_{M_T} - \mathbf{H}^H(t)\mathbf{H}(t))(\hat{\mathbf{s}}^t - \mathbf{s}_0)$ , the real and imaginary parts are normally

distributed with zero mean and variance  $\frac{\|\hat{\mathbf{s}}^t - \mathbf{s}_0\|_2^2}{2M_R} + \delta_\ell^t$  and  $\frac{\|\hat{\mathbf{s}}^t - \mathbf{s}_0\|_2^2}{2M_R} - \delta_\ell^t$  respectively, with  $\delta_\ell^t = \frac{\text{Re}\{(\hat{s}_\ell^t - s_{0\ell})^2\}}{2M_R}$ . With

$$\hat{\sigma}_t^2 = \lim_{M_T \rightarrow \infty} \|\hat{\mathbf{s}}^t - \mathbf{s}_0\|^2 / M_T, \quad (54)$$

and noting that  $\delta_\ell^t \rightarrow 0$  as  $M_T \rightarrow \infty$ , we have that

$$(\mathbf{I}_{M_T} - \mathbf{H}^H(t)\mathbf{H}(t))(\hat{\mathbf{s}}^t - \mathbf{s}_0) \rightarrow \mathcal{CN}(0, \beta\hat{\sigma}_t^2).$$

Moreover, by conditioning on  $\mathbf{n}$ ,  $\mathbf{H}^H(t)\mathbf{n} \rightarrow \mathcal{CN}(0, N_0)$  by the law of large numbers. By Definition 3 of the effective noise variance of cB-AMP, we have the relation  $\sigma_t^2 = N_0 + \beta\hat{\sigma}_t^2$  with  $\hat{\sigma}_t^2$  defined in (54). Thus, each  $\ell$ th entry of (51) converges to  $F(s_{0\ell} + \sigma_t Z, N_0^{\text{post}}(1 + \tau^t))$  where  $Z \sim \mathcal{CN}(0, 1)$ . Since we assume a fixed prior distribution for all  $s_{0\ell}$ , we obtain the following recursion for (51):

$$\begin{aligned} \sigma_{t+1}^2 &= N_0 + \beta \lim_{M_T \rightarrow \infty} \frac{1}{M_T} \|\hat{\mathbf{s}}^{t+1} - \mathbf{s}_0\|^2 \\ &= N_0 + \beta \mathbb{E}_{S,Z} \left[ |F(S + \sigma_t Z, N_0^{\text{post}}(1 + \tau^t)) - S|^2 \right], \end{aligned}$$

with  $S \sim p(S)$ . Starting from (52), we use (53) and (54), and the law of large numbers to obtain:

$$\begin{aligned} \tau^{t+1} &= \frac{\beta}{N_0^{\text{post}}} \langle \mathbf{G}(\hat{\mathbf{s}}^t + \mathbf{H}^H(t)\mathbf{r}^t, N_0^{\text{post}}(1 + \tau^t)) \rangle \\ &= \frac{\beta}{N_0^{\text{post}}} \mathbb{E}_{S,Z} [\mathbf{G}(S + \sigma_t Z, N_0^{\text{post}}(1 + \tau^t))]. \end{aligned}$$

By introducing the postulated variance  $\gamma_t^2 = N_0^{\text{post}}(1 + \tau^t)$ , we obtain the final cSE:

$$\begin{aligned} \sigma_{t+1}^2 &= N_0 + \beta \mathbb{E}_{S,Z} \left[ |F(S + \sigma_t Z, \gamma_t^2) - S|^2 \right] \\ \gamma_{t+1}^2 &= N_0^{\text{post}} + \beta \mathbb{E}_{S,Z} [\mathbf{G}(S + \sigma_t Z, \gamma_t^2)]. \end{aligned}$$

We reiterate that the formulation of  $\mathbf{H}(t)$  to obtain cSE in Theorem 1 was non-rigorous; a rigorous proof can be found in [29].

## APPENDIX E

### PROOF OF LEMMA 2

We start with cB-AMP as detailed in Algorithm 1. We simplify intermediate steps in cB-AMP using the definition of  $F(\hat{s}_\ell, \tau)$  and  $G(\hat{s}_\ell, \tau)$ , and our knowledge of the prior distribution. Recall that  $F(\hat{s}_\ell, \tau)$  in (20) was defined as

$$F(\hat{s}_\ell, \tau) = \sum_{a \in \mathcal{O}} w_a(\hat{s}_\ell, \tau) a,$$

By taking partial derivatives of  $F(\hat{s}_\ell, \tau)$  with the notations defined in Algorithm 1, we have the following expressions, where we drop the notation  $w_a = w_a(\hat{s}_\ell, \tau)$  for simplicity.

$$\begin{aligned}\partial_1 F^{\text{R}} &= \frac{2}{\tau} \left[ \sum_{a \in \mathcal{O}} \text{Re}\{a\}^2 w_a - \left( \sum_{a \in \mathcal{O}} \text{Re}\{a\} w_a \right)^2 \right], \\ \partial_2 F^{\text{I}} &= \frac{2}{\tau} \left[ \sum_{a \in \mathcal{O}} \text{Im}\{a\}^2 w_a - \left( \sum_{a \in \mathcal{O}} \text{Im}\{a\} w_a \right)^2 \right], \\ \partial_2 F^{\text{I}} = \partial_1 F^{\text{R}} &= \frac{2}{\tau} \left[ \sum_{a \in \mathcal{O}} \text{Re}\{a\} \text{Im}\{a\} w_a \right. \\ &\quad \left. - \left( \sum_{a \in \mathcal{O}} \text{Re}\{a\} w_a \right) \left( \sum_{a \in \mathcal{O}} \text{Im}\{a\} w_a \right) \right].\end{aligned}$$

Note that (21) can be separated in real and imaginary parts. Therefore,

$$\begin{aligned}\mathsf{G}(\hat{s}_\ell, \tau) &= \sum_{a \in \mathcal{O}} |a|^2 w_a - \left| \sum_{a \in \mathcal{O}} a w_a \right|^2 \\ &= \sum_{a \in \mathcal{O}} \text{Re}\{a\}^2 w_a - \left( \sum_{a \in \mathcal{O}} \text{Re}\{a\} w_a \right)^2 \\ &\quad + \sum_{a \in \mathcal{O}} \text{Im}\{a\}^2 w_a - \left( \sum_{a \in \mathcal{O}} \text{Im}\{a\} w_a \right)^2 \\ &= \frac{\tau}{2} [\partial_1 F^{\text{R}} + \partial_2 F^{\text{I}}](\hat{s}_\ell, \tau)\end{aligned}$$

Finally, observe that  $\partial_1 F^{\text{I}} = \partial_2 F^{\text{R}}$  and  $1/i = -i$ , so Lemma 2 simplifies to:

$$\begin{aligned}\hat{\mathbf{s}}^{t+1} &= \mathsf{F}(\hat{\mathbf{s}}^t + \mathbf{H}^{\text{H}} \mathbf{r}^t, N_0^{\text{post}}(1 + \tau^t)) \\ \tau^{t+1} &= \frac{\beta}{N_0^{\text{post}}} \langle \mathsf{G}(\hat{\mathbf{s}}^t + \mathbf{H}^{\text{H}} \mathbf{r}^t, N_0^{\text{post}}(1 + \tau^t)) \rangle \\ \mathbf{r}^{t+1} &= \mathbf{y} - \mathbf{H} \hat{\mathbf{s}}^{t+1} + \frac{\tau^{t+1}}{1 + \tau^t} \mathbf{r}^t.\end{aligned}$$

## APPENDIX F

### PROOF OF LEMMA 3

Since  $N_0^{\text{post}} \rightarrow \infty$ , the recursions in Algorithm 2 are given by

$$\begin{aligned}\hat{\mathbf{s}}^t &= \lim_{N_0^{\text{post}} \rightarrow \infty} \mathsf{F}(\hat{\mathbf{s}}^{t-1} + \mathbf{H}^{\text{H}} \mathbf{r}^{t-1}, N_0^{\text{post}}), \\ \mathbf{r}^t &= \mathbf{y} - \mathbf{H} \hat{\mathbf{s}}^t.\end{aligned}$$

First of all, notice that as  $N_0^{\text{post}} \rightarrow \infty$ ,  $w_a(\hat{s}_\ell, N_0^{\text{post}}) \rightarrow p_a$  for any  $\hat{s}_\ell$ . Therefore, for all  $t$ ,

$$\begin{aligned}\hat{\mathbf{s}}^t &= \lim_{N_0^{\text{post}} \rightarrow \infty} \mathbf{F}(\hat{\mathbf{s}}^{t+1} + \mathbf{H}^H \mathbf{r}^{t-1}, N_0^{\text{post}}) \rightarrow \sum_{a \in \mathcal{O}} a p_a = 0, \\ \mathbf{r}^t &= \mathbf{y} - \mathbf{H} \hat{\mathbf{s}}^t = \mathbf{y},\end{aligned}$$

and thus, the Gaussian output  $\mathbf{z}^t = \hat{\mathbf{s}}^t + \mathbf{H}^H \mathbf{r}^t$  is equivalent to the matched filter output  $\mathbf{H}^H \mathbf{y}$ . To show that the non-linear MMSE output corresponds to the matched filter involves computing  $\lim_{N_0^{\text{post}} \rightarrow \infty} \frac{N_0^{\text{post}}}{E_s} \hat{\mathbf{s}}^{t+1}$ , which is given by

$$\begin{aligned}\lim_{N_0^{\text{post}} \rightarrow \infty} \frac{N_0^{\text{post}}}{E_s} \hat{\mathbf{s}}^{t+1} &= \lim_{N_0^{\text{post}} \rightarrow \infty} \frac{N_0^{\text{post}}}{E_s} \mathbf{F}(\mathbf{H}^H \mathbf{y}, N_0^{\text{post}}) \\ &= \lim_{N_0^{\text{post}} \rightarrow \infty} \frac{N_0^{\text{post}}}{E_s} \sum_{a \in \mathcal{O}} a p_a \left( 1 - \frac{1}{N_0^{\text{post}}} |\mathbf{H}^H \mathbf{y} - a|^2 \right) \\ &= -\frac{1}{E_s} \sum_{a \in \mathcal{O}} a p_a |\mathbf{H}^H \mathbf{y} - a|^2 = \mathbf{H}^H \mathbf{y}.\end{aligned}$$

## APPENDIX G

### PROOF OF LEMMA 4

First, note that as  $\beta \rightarrow 0$  for a fixed  $N_0^{\text{post}}$ , we have that  $\tau^t = 0$  for all  $t \geq 1$ . Therefore, we have the following recursions,

$$\begin{aligned}\hat{\mathbf{s}}^{t+1} &= \mathbf{F}(\hat{\mathbf{s}}^t + \mathbf{H}^H \mathbf{r}^t, N_0^{\text{post}}), \\ \mathbf{r}^{t+1} &= \mathbf{y} - \mathbf{H} \hat{\mathbf{s}}^{t+1}.\end{aligned}$$

Following the derivation of complex state evolution in Appendix D, as  $\beta \rightarrow 0$ , we have

$$\hat{\mathbf{s}}^t + \mathbf{H}^H \mathbf{r}^t = \mathbf{H}^H \mathbf{y} + (\mathbf{I}_{M_T} - \mathbf{H}^H \mathbf{H}) \hat{\mathbf{s}}^t \rightarrow \mathbf{H}^H \mathbf{y},$$

because the entries of  $(\mathbf{I}_{M_T} - \mathbf{H}^H \mathbf{H}) \hat{\mathbf{s}}^t$  converge to a complex normal distribution with zero mean and variance  $\beta \tilde{\sigma}_t^2$  with  $\tilde{\sigma}_t^2 = \lim_{M_T \rightarrow \infty} \frac{1}{M_T} \|\hat{\mathbf{s}}^t\|^2$ . Since  $\tilde{\sigma}_t^2$  is finite and  $\beta \rightarrow 0$ , we have that the Gaussian output of LAMA is  $\mathbf{z}^t = \mathbf{H}^H \mathbf{y}$  (independent of the iteration index  $t$ ). Hence, the non-linear MMSE output  $\hat{\mathbf{s}}^{t+1}$  of LAMA is given by  $\mathbf{F}(\mathbf{H}^H \mathbf{y}, N_0^{\text{post}})$  for all  $t$ .

We show that one iteration of LAMA is sufficient to achieve AWGN performance by the cSE in Theorem 1. Recall that previous paragraph demonstrated that  $\mathbf{z}^t = \mathbf{H}^H \mathbf{y}$  for all  $t$ . Thus, the equivalent output noise variance is computed as  $\sigma^2 = N_0 + \beta \text{Var}_S[S] = N_0$ , where the last step comes from  $\beta \rightarrow 0$ . Since each output of LAMA is identical every iteration and the output noise variance is  $N_0$ , one iteration is sufficient to achieve AWGN performance.

## APPENDIX H

## PROOF OF LEMMA 5

Note that since  $N_0 = 0$ , we have  $\sigma^2 = \gamma^2$  by Corollary 2. Since the variance of  $S$  is finite, denote  $\text{Var}_S[S] = \sigma_s^2$ . By [90, Prop. 15], we have the following upper bound for  $\Psi(\sigma^2, \sigma^2)$ :

$$\Psi(\sigma^2, \sigma^2) \leq \frac{\sigma_s^2}{\sigma_s^2 + \sigma^2} \sigma^2, \quad (55)$$

where equality is achieved for all  $\sigma^2$  if and only if  $S$  is complex normal with variance  $\sigma_s^2$ . Note that if  $\sigma^2 = 0$ , then (55) is achieved for any  $\sigma_s^2$ . If  $\sigma^2 > 0$ , then

$$\Psi(\sigma^2, \sigma^2) \leq \frac{\sigma_s^2}{\sigma_s^2 + \sigma^2} \sigma^2 = \frac{1}{1 + \sigma^2/\sigma_s^2} \sigma^2 < \sigma^2,$$

and, hence, the proof follows.

The first part of Lemma 5 is trivial from (55), and thus,  $\Psi(\sigma^2, \sigma^2) \rightarrow 0$  as  $\sigma^2 \rightarrow 0$ . The second part is noting that as  $\sigma^2 \rightarrow \infty$ ,  $F(\cdot, \sigma^2) \rightarrow \sum_{a \in \mathcal{O}} a p_a = \mathbb{E}_S[S]$ , and hence we have

$$\lim_{\sigma^2 \rightarrow \infty} \Psi(\sigma^2, \sigma^2) \rightarrow \mathbb{E}_S[|S - \mathbb{E}_S[S]|^2] = \text{Var}_S[S].$$

## APPENDIX I

## PROOF OF THEOREM 5

We assume the initialization in Algorithm 2. Since  $N_0 = N_0^{\text{post}} = 0$ , if LAMA perfectly recovers the true signal  $\mathbf{s}_0$ , then the fixed-point (31) is unique at  $\sigma^2 = 0$ . This happens if the system ratio is strictly less than the ERT,  $\beta_{\mathcal{O}}^{\text{max}}$  because otherwise, i.e.,  $\beta \geq \beta_{\mathcal{O}}^{\text{max}}$ , there exists a non-unique fixed point to (31) for some  $\sigma^2 > 0$  by Definition 6.

## APPENDIX J

## PROOF OF LEMMA 6

We show that for a fixed constellation  $\mathcal{O}$ ,  $\beta_{\mathcal{O}}^{\text{min}} \leq \beta_{\mathcal{O}}^{\text{max}}$ . For conciseness, define  $\sigma_*^2$  as the fixed-point  $\sigma^2 = \beta_{\mathcal{O}}^{\text{max}} \Psi(\sigma^2, \sigma^2)$ . The proof is straightforward as,

$$\begin{aligned} \beta_{\mathcal{O}}^{\text{min}} &\stackrel{(a)}{=} \min_{\sigma^2 > 0} \left\{ \left( \frac{d\Psi(\sigma^2, \sigma^2)}{d\sigma^2} \right)^{-1} \right\} \leq \left( \frac{d\Psi(\sigma^2, \sigma^2)}{d\sigma^2} \right)^{-1} \Big|_{\sigma^2 = \sigma_*^2} \\ &\stackrel{(b)}{=} \left( \frac{1}{\beta_{\mathcal{O}}^{\text{max}}} \right)^{-1} = \beta_{\mathcal{O}}^{\text{max}}, \end{aligned}$$

where (a) and (b) follow from the definitions of MRT and ERT, respectively.



## APPENDIX K

## PROOF OF LEMMA 7

As  $\beta < \beta_{\mathcal{O}}^{\max}$ , there exists a value of  $N_0$ , denote it as  $N_0^*$ , such that for  $N_0 < N_0^*$ , the fixed-point solution of LAMA is unique. We note that  $N_0^{\min}(\beta)$  is also a candidate for  $N_0^*$  as the fixed-point solution of LAMA is unique for all  $N_0 < N_0^{\min}(\beta)$ . In addition, since  $\mathcal{O}$  is a constellation, by [58, Thm. 10],  $\Psi(\sigma^2, \sigma^2)$  has a continuous derivative and  $\lim_{\sigma^2 \rightarrow 0} \frac{d}{d\sigma^2} \Psi(\sigma^2, \sigma^2) = 0$ . Hence, there exists a value  $\sigma_*^2$  such that for all  $\sigma^2 < \sigma_*^2$ ,

$$\frac{d}{d\sigma^2} \Psi(\sigma^2, \sigma^2) < \frac{1}{2\beta}. \quad (56)$$

Now, suppose that  $N_0^* < \sigma_*^2/2$ . Then, for all  $\sigma^2 < \sigma_*^2$  we have:

$$N_0 + \beta \Psi(\sigma^2, \sigma^2) \stackrel{(a)}{<} N_0 + \frac{\sigma^2}{2},$$

where (a) follows from (56) and the mean value theorem. Since  $2N_0 < 2N_0^* < \sigma_*^2$ , we have that:

$$N_0 + \beta \Psi(2N_0, 2N_0) < N_0 + N_0 = 2N_0,$$

and therefore, the fixed-point solution  $\sigma^2$  has to be between  $N_0$  and  $2N_0$ . As a result, as  $N_0 \rightarrow 0$ , the fixed-point solution  $\sigma^2 \rightarrow 0$ . The last part is apparent as:

$$\begin{aligned} \lim_{N_0 \rightarrow 0} 1 &= \lim_{N_0 \rightarrow 0} \frac{N_0}{\sigma^2} + \beta \lim_{N_0 \rightarrow 0} \frac{\Psi(\sigma^2, \sigma^2)}{\sigma^2} \\ &= \lim_{N_0 \rightarrow 0} \frac{N_0}{\sigma^2} + \beta \lim_{\sigma^2 \rightarrow 0} \frac{d}{d\sigma^2} \Psi(\sigma^2, \sigma^2) = \lim_{N_0 \rightarrow 0} \frac{N_0}{\sigma^2}, \end{aligned}$$

## APPENDIX L

## PROOF OF LEMMA 8

Since the constellation  $\mathcal{O}$  is separable, we introduce a shorthand notation for  $\mathcal{O}^{\text{R}} = \text{Re}\{\mathcal{O}\}$  and  $\mathcal{O}^{\text{I}} = \text{Im}\{\mathcal{O}\}$ . It is easy to observe that the weight scalar  $w_a(\hat{s}_\ell, \tau)$  can be rewritten as a product between the weight scalar of the real and imaginary constellation  $w_{a_{\text{R}}}(\hat{s}_\ell, \tau)$  and  $w_{a_{\text{I}}}(\hat{s}_\ell, \tau)$ , i.e.,  $w_a(\hat{s}_\ell, \tau) = w_{a_{\text{R}}}(\hat{s}_\ell, \tau)w_{a_{\text{I}}}(\hat{s}_\ell, \tau)$  where

$$w_{a_{\text{R}}}(\hat{s}_\ell, \tau) = \frac{p_{a_{\text{R}}} \exp\left(-\frac{1}{\tau}(\text{Re}\{\hat{s}_\ell\} - a_{\text{R}})^2\right)}{\sum_{a_{\text{R}} \in \mathcal{O}^{\text{R}}} p_{a_{\text{R}}} \exp\left(-\frac{1}{\tau}(\text{Re}\{\hat{s}_\ell\} - a_{\text{R}})^2\right)}, \quad (57)$$

and likewise for  $w_{a_{\text{I}}}$ . Therefore,  $\mathbf{F}$  is separable because

$$\mathbf{F}(\hat{s}_\ell, \tau) = \sum_{a \in \mathcal{O}} w_a(\hat{s}_\ell, \tau) a$$

$$\begin{aligned}
&= \sum_{a \in \mathcal{O}} w_a(\hat{s}_\ell, \tau) a_{\text{R}} + i \sum_{a \in \mathcal{O}} w_a(\hat{s}_\ell, \tau) a_{\text{I}} \\
&= \sum_{a_{\text{R}} \in \mathcal{O}^{\text{R}}} a_{\text{R}} \sum_{a_{\text{I}} \in \mathcal{O}^{\text{I}}} w_a(\hat{s}_\ell, \tau) + i \sum_{a_{\text{I}} \in \mathcal{O}^{\text{I}}} a_{\text{I}} \sum_{a_{\text{R}} \in \mathcal{O}^{\text{R}}} w_a(\hat{s}_\ell, \tau) \\
&= \sum_{a_{\text{R}} \in \mathcal{O}^{\text{R}}} w_{a_{\text{R}}}(\hat{s}_\ell, \tau) a_{\text{R}} + i \sum_{a_{\text{I}} \in \mathcal{O}^{\text{I}}} w_{a_{\text{I}}}(\hat{s}_\ell, \tau) a_{\text{I}}.
\end{aligned} \tag{58}$$

Now, for a real-valued constellation  $\mathcal{O}^{\text{R}}$ , the message mean  $F^{\text{R}}$  is given by:

$$F^{\text{R}}(\hat{s}_\ell, \tau) = \sum_{a \in \mathcal{O}^{\text{R}}} w_a^{\text{R}}(\hat{s}_\ell, \tau) a, \tag{59}$$

where the weight scalar for the real-valued constellation is computed by

$$w_a^{\text{R}}(\hat{s}_\ell, \tau) = \frac{p_a \exp\left(-\frac{1}{2\tau}(\hat{s}_\ell - a)^2\right)}{\sum_{a \in \mathcal{O}^{\text{R}}} p_a \exp\left(-\frac{1}{2\tau}(\hat{s}_\ell - a)^2\right)}.$$

Therefore, we have that:

$$\begin{aligned}
\Psi(\sigma^2, \gamma^2) &= \mathbb{E}_{S, Z} \left[ |F(S + \sigma Z, \gamma^2) - S|^2 \right] \\
&\stackrel{(a)}{=} \mathbb{E}_{S_{\text{R}}, Z_{\text{R}}} \left[ \left( \text{Re} \left\{ F\left(S_{\text{R}} + \frac{\sigma}{\sqrt{2}} Z_{\text{R}}, \gamma^2\right) \right\} - S_{\text{R}} \right)^2 \right] \\
&\quad + \mathbb{E}_{S_{\text{I}}, Z_{\text{I}}} \left[ \left( \text{Im} \left\{ F\left(S_{\text{I}} + \frac{\sigma}{\sqrt{2}} Z_{\text{I}}, \gamma^2\right) \right\} - S_{\text{I}} \right)^2 \right] \\
&\stackrel{(b)}{=} 2 \mathbb{E}_{S_{\text{R}}, Z_{\text{R}}} \left[ \left( \text{Re} \left\{ F\left(S_{\text{R}} + \frac{\sigma}{\sqrt{2}} Z_{\text{R}}, \gamma^2\right) \right\} - S_{\text{R}} \right)^2 \right] \\
&\stackrel{(c)}{=} 2 \mathbb{E}_{S_{\text{R}}, Z_{\text{R}}} \left[ \left( \sum_{a \in \mathcal{O}^{\text{R}}} w_a^{\text{R}}\left(S_{\text{R}} + \frac{\sigma}{\sqrt{2}} Z_{\text{R}}, \frac{\gamma^2}{2}\right) a - S_{\text{R}} \right)^2 \right] \\
&= 2\Psi^{\text{R}}\left(\frac{\sigma^2}{2}, \frac{\sigma^2}{2}\right),
\end{aligned}$$

where (a) follows from (58), (b) from definition of separable constellation, and (c) follows from construction of (59). We note that the case for variance function  $\Phi$  is derived similarly.

## APPENDIX M

### PROOF OF LEMMA 9

We show that for a separable constellation  $\mathcal{O}$ , the MRT and ERT are equivalent. Denote the complex-valued MSE function as  $\Psi(\sigma^2, \sigma^2) = \mathbb{E}_{S, Z} \left[ |F(S + \sigma Z, \sigma^2) - S|^2 \right]$ , where  $Z \sim \mathcal{CN}(0, 1)$ , and  $S \sim p(S)$  for constellation  $\mathcal{O}$ . Denote the real-valued MSE function  $\Psi^{\text{R}}(\sigma^2, \sigma^2) = \mathbb{E}_{S_{\text{R}}, Z^{\text{R}}} \left[ (F(S_{\text{R}} + \sigma Z^{\text{R}}, \sigma^2) - S_{\text{R}})^2 \right]$ , where  $Z^{\text{R}} \sim \mathcal{N}(0, 1)$  and  $S_{\text{R}} \sim p(S_{\text{R}})$  for the real-valued

constellation  $\text{Re}\{\mathcal{O}\}$ . We know from Lemma 8 that  $\Psi(\sigma^2, \sigma^2) = 2\Psi^{\text{R}}(\sigma^2/2, \sigma^2/2)$ . By denoting  $\beta_{\mathcal{C}}^{\min}$  and  $\beta_{\mathbb{R}}^{\min}$  as the MRT of complex- and real-valued MSE function, respectively, we have:

$$\begin{aligned}\beta_{\mathcal{C}}^{\min} &= \min_{\sigma^2 \geq 0} \left\{ \left( \frac{\text{d}\Psi(\sigma^2, \sigma^2)}{\text{d}\sigma^2} \right)^{-1} \right\} \\ &= \min_{\sigma^2 \geq 0} \left\{ \left( \frac{\text{d}\Psi^{\text{R}}(\frac{\sigma^2}{2}, \frac{\sigma^2}{2})}{\text{d}\sigma^2/2} \right)^{-1} \right\} \\ &= \min_{\bar{\sigma}^2 \geq 0} \left\{ \left( \frac{\text{d}\Psi^{\text{R}}(\bar{\sigma}^2, \bar{\sigma}^2)}{\text{d}\bar{\sigma}^2} \right)^{-1} \right\} \\ &= \beta_{\mathbb{R}}^{\min}\end{aligned}$$

The remaining quantities,  $\beta^{\max}$  and the critical noise levels of Lemma 9 can be derived similarly.

## APPENDIX N

### PROOF OF LEMMA 10

Note that if  $\beta < \beta_{\mathcal{O}}^{\min}$ , then the slope of the function  $\beta\Psi(\sigma^2, \sigma^2)$  with respect to  $\sigma^2$  is always less than 1, i.e.,  $\beta \frac{\text{d}}{\text{d}\sigma^2} \Psi(\sigma^2, \sigma^2) \Big|_{\sigma^2=\sigma_*^2} < 1$  for any  $\sigma_*^2 > 0$ . In addition, since  $\beta < \beta_{\mathcal{O}}^{\min}$ , the fixed-point solution to  $N_0 + \beta\Psi(\sigma^2, \sigma^2) = \sigma^2$  is unique. Now the exponentially-fast convergence result can be shown by using the bounding technique of [30, Lem. 6.4.1].

In [30], the proof for showing exponentially-fast convergence of standard AMP to its largest fixed-point solution was shown by analyzing the stability constant  $\text{SC}(\Psi)$  which was defined by:

$$\begin{aligned}\text{SC}(\Psi) &= \beta \frac{\text{d}}{\text{d}\sigma^2} \Psi(\sigma^2, \sigma^2) \Big|_{\sigma^2=\sigma_*^2}, \\ \sigma_*^2 &= \max_{\sigma^2 > 0} \{ \sigma^2 : N_0 + \beta\Psi(\sigma^2, \sigma^2) \geq \sigma^2 \}\end{aligned}$$

Using the new notation of stability constant, the condition of  $\text{SC}(\Psi) < 1$ , i.e., slope at the largest fixed point is less than 1, was only needed in [30] to show exponential-fast convergence. However, we note that this approach was viable in [30] due to concavity of the MSE function of  $\Psi(\sigma^2, \sigma^2)$  for the soft-thresholding function; however, the MSE function of LAMA does not have such properties. In fact, the MSE function for LAMA for commonly used constellation in wireless is neither convex nor concave. However, as shown above, if  $\beta < \beta_{\mathcal{O}}^{\min}$ , we have that not only  $\text{SC}(\Psi) < 1$ , but also  $\beta \frac{\text{d}}{\text{d}\sigma^2} \Psi(\sigma^2, \sigma^2) \Big|_{\sigma^2=\sigma_*^2} < 1$  for any  $\sigma_*^2 > 0$ . Therefore, if  $\beta < \beta_{\mathcal{O}}^{\min}$ , LAMA converges exponentially fast to its unique fixed-point solution  $\sigma_*^2$ .

## REFERENCES

- [1] C. Jeon, R. Ghods, A. Maleki, and C. Studer, "Optimality of large MIMO detection via approximate message passing," in *Proc. IEEE Int. Symp. Inf. Theory (ISIT)*, Jun. 2015, pp. 1227–1231.
- [2] D. Guo and S. Verdú, "Multiuser detection and statistical mechanics," in *Commun., Inf. and Netw. Security*. Springer, 2003, pp. 229–277.
- [3] —, "Randomly spread CDMA: Asymptotics via statistical physics," *IEEE Trans. Inf. Theory*, vol. 51, no. 6, pp. 1983–2010, Jun. 2005.
- [4] F. Rusek, D. Persson, B. K. Lau, E. G. Larsson, T. L. Marzetta, O. Edfors, and F. Tufvesson, "Scaling up MIMO: Opportunities and challenges with very large arrays," *IEEE Signal Process. Mag.*, vol. 30, no. 1, pp. 40–60, Jan. 2013.
- [5] E. Larsson, O. Edfors, F. Tufvesson, and T. Marzetta, "Massive MIMO for next generation wireless systems," *IEEE Commun. Mag.*, vol. 52, no. 2, pp. 186–195, Feb. 2014.
- [6] J. Andrews, S. Buzzi, W. Choi, S. Hanly, A. Lozano, A. Soong, and J. Zhang, "What will 5G be?" *IEEE J. Sel. Areas Commun.*, vol. 32, no. 6, pp. 1065–1082, Jun. 2014.
- [7] T. L. Marzetta, "Non-cooperative cellular wireless with unlimited numbers of base station antennas," *IEEE Trans. Wireless Comm.*, vol. 9, no. 11, pp. 3590–3600, Nov. 2010.
- [8] J. Hoydis, S. ten Brink, and M. Debbah, "Massive MIMO: How many antennas do we need?" in *Proc. Allerton Conf. Commun., Contr., Comput.*, Sept. 2011, pp. 545–550.
- [9] M. Wu, B. Yin, A. Vosoughi, C. Studer, J. Cavallaro, and C. Dick, "Approximate matrix inversion for high-throughput data detection in the large-scale MIMO uplink," in *Proc. IEEE Int. Symp. Circuits and Syst. (ISCAS)*, May 2013, pp. 2155–2158.
- [10] M. Wu, B. Yin, G. Wang, C. Dick, J. Cavallaro, and C. Studer, "Large-scale MIMO detection for 3GPP LTE: Algorithm and FPGA implementation," *IEEE J. Sel. Topics Signal Process.*, vol. 8, no. 5, pp. 916–929, Oct. 2014.
- [11] W. C. Y. Lee, "Overview of cellular CDMA," *IEEE Trans. Veh. Technol.*, vol. 40, no. 2, pp. 291–302, May 1991.
- [12] A. J. Viterbi, *CDMA: Principles of Spread Spectrum Communication*. Addison Wesley Longman Publishing Co., Inc., 1995.
- [13] K. Gilhousen, I. Jacobs, R. Padovani, A. Viterbi, J. Weaver, L.A., and I. Wheatley, C.E., "On the capacity of a cellular CDMA system," *IEEE Trans. Veh. Technol.*, vol. 40, no. 2, pp. 303–312, May 1991.
- [14] S. Hara and R. Prasad, "Overview of multicarrier CDMA," *IEEE Commun. Mag.*, vol. 35, no. 12, pp. 126–133, Dec 1997.
- [15] R. Lupas and S. Verdú, "Linear multiuser detectors for synchronous code-division multiple-access channels," *IEEE Trans. Inf. Theory*, vol. 35, no. 1, pp. 123–136, Jan. 1989.
- [16] T. Tanaka, "A statistical-mechanics approach to large-system analysis of CDMA multiuser detectors," *IEEE Trans. Inf. Theory*, vol. 48, no. 11, pp. 2888–2910, Nov. 2002.
- [17] Y. Kabashima, "A CDMA multiuser detection algorithm on the basis of belief propagation," *J. Phys. A: Math. Gen.*, vol. 36, no. 43, pp. 11 111–11 121, Oct. 2003.
- [18] A. B. Brown, "Linear diophantine equations," *Math. Mag.*, vol. 31, no. 4, pp. 215–220, 1958.
- [19] E. Contejean and H. Devie, "An efficient incremental algorithm for solving systems of linear diophantine equations," *Inform. Comput.*, vol. 113, no. 1, pp. 143–172, Aug. 1994.
- [20] U. Fincke and M. Pohst, "Improved methods for calculating vectors of short length in a lattice, including a complexity analysis," *Math. Comp.*, vol. 44, no. 170, pp. 463–471, Apr. 1985.
- [21] E. Agrell, T. Eriksson, A. Vardy, and K. Zeger, "Closest point search in lattices," *IEEE Trans. Inf. Theory*, vol. 48, no. 8, pp. 2201–2214, Aug. 2002.

- [22] S. Verdú and S. Shamai, “Spectral efficiency of CDMA with random spreading,” *IEEE Trans. Inf. Theory*, vol. 45, no. 2, pp. 622–640, Mar. 1999.
- [23] M. Mézard, G. Parisi, and M. A. Virasoro, *Spin Glass Theory and Beyond*. Singapore: World Scientific, 1987.
- [24] A. Montanari and D. Tse, “Analysis of belief propagation for non-linear problems: The example of CDMA (or: How to prove Tanaka’s formula),” in *Proc. IEEE Inf. Theory Workshop (ITW)*, March 2006, pp. 160–164.
- [25] D. Guo and C.-C. Wang, “Asymptotic mean-square optimality of belief propagation for sparse linear systems,” in *Proc. IEEE Inf. Theory Workshop (ITW)*, Oct. 2006, pp. 194–198.
- [26] ———, “Random sparse linear systems observed via arbitrary channels: A decoupling principle,” in *Proc. IEEE Int. Symp. Inf. Theory (ISIT)*, 2007, pp. 946–950.
- [27] G. Caire, R. Müller, and T. Tanaka, “Iterative multiuser joint decoding: optimal power allocation and low-complexity implementation,” *IEEE Trans. Inf. Theory*, vol. 50, no. 9, pp. 1950–1973, Sept. 2004.
- [28] D. Donoho, A. Maleki, and A. Montanari, “Message-passing algorithms for compressed sensing,” *Proc. Natl. Academy of Sciences (PNAS)*, vol. 106, no. 45, pp. 18 914–18 919, Sept. 2009.
- [29] M. Bayati and A. Montanari, “The dynamics of message passing on dense graphs, with applications to compressed sensing,” *IEEE Trans. Inf. Theory*, vol. 57, no. 2, pp. 764–785, Feb. 2011.
- [30] A. Maleki, “Approximate message passing algorithms for compressed sensing,” Ph.D. dissertation, Stanford University, Jan. 2011.
- [31] D. Donoho, “Compressed sensing,” *IEEE Trans. Inf. Theory*, vol. 52, no. 1, pp. 1289–1306, Jan. 2006.
- [32] E. Candès and M. Wakin, “An introduction to compressive sampling,” *IEEE Signal Process. Mag.*, vol. 25, no. 2, pp. 21–30, Mar. 2008.
- [33] C. A. Metzler, A. Maleki, and R. G. Baraniuk, “From Denoising to Compressed Sensing,” *IEEE Trans. Inf. Theory*, vol. 62, no. 9, pp. 5117–5144, 2016.
- [34] A. Montanari, *Graphical models concepts in compressed sensing, Compressed Sensing (Y.C. Eldar and G. Kutyniok, eds.)*. Cambridge University Press, 2012.
- [35] D. Donoho, A. Maleki, and A. Montanari, “Message passing algorithms for compressed sensing: I. Motivation and construction,” in *Proc. IEEE Inf. Theory Workshop (ITW)*, Jan. 2010, pp. 1–5.
- [36] ———, “Message passing algorithms for compressed sensing: II. Analysis and validation,” in *Proc. IEEE Inf. Theory Workshop (ITW)*, Jan. 2010, pp. 1–5.
- [37] A. Maleki, L. Anitori, Z. Yang, and R. Baraniuk, “Asymptotic analysis of complex LASSO via complex approximate message passing (CAMP),” *IEEE Trans. Inf. Theory*, vol. 59, no. 7, pp. 4290–4308, Jul. 2013.
- [38] S. Rangan, “Generalized approximate message passing for estimation with random linear mixing,” *arXiv:1010.5141*, 2010.
- [39] A. Javanmard and A. Montanari, “State evolution for general approximate message passing algorithms, with applications to spatial coupling,” *J. Inf. Inference*, vol. 2, no. 2, pp. 115–144, Oct. 2013.
- [40] S. Rangan, P. Schniter, and A. K. Fletcher, “Vector approximate message passing,” in *Proc. IEEE Int. Symp. Inf. Theory (ISIT)*, Jun. 2017, pp. 1588–1592.
- [41] J. Vila and P. Schniter, “Expectation-maximization gaussian-mixture approximate message passing,” *IEEE Trans. Signal Process.*, vol. 61, no. 19, pp. 4658–4672, Oct. 2013.
- [42] U. Kamilov, S. Rangan, A. Fletcher, and M. Unser, “Approximate message passing with consistent parameter estimation and applications to sparse learning,” *IEEE Trans. Inf. Theory*, vol. 60, no. 5, pp. 2969–2985, May 2014.
- [43] S. Rangan, P. Schniter, E. Riegler, A. Fletcher, and V. Cevher, “Fixed points of generalized approximate message passing with arbitrary matrices,” in *Proc. IEEE Int. Symp. Inf. Theory (ISIT)*, Jul. 2013, pp. 664–668.

- [44] J. Vila and P. Schniter, "Expectation-maximization bernoulli-gaussian approximate message passing," in *Proc. Asilomar Conf. Signals, Syst., Comput.*, Nov. 2011, pp. 799–803.
- [45] U. Kamilov, V. Goyal, and S. Rangan, "Message-passing de-quantization with applications to compressed sensing," *IEEE Trans. Signal Process.*, vol. 60, no. 12, pp. 6270–6281, Dec. 2012.
- [46] P. Maechler, C. Studer, D. E. Bellasi, A. Maleki, A. Burg, N. Felber, H. Kaeslin, and R. G. Baraniuk, "VLSI design of approximate message passing for signal restoration and compressive sensing," *IEEE J. Emerg. Sel. Topics Circuits Syst.*, vol. 2, no. 3, pp. 579–590, Sep. 2012.
- [47] S. Som and P. Schniter, "Compressive imaging using approximate message passing and a markov-tree prior," *IEEE Trans. Signal Process.*, vol. 60, no. 7, pp. 3439–3448, Jul. 2012.
- [48] P. Schniter and S. Rangan, "Compressive phase retrieval via generalized approximate message passing," in *Proc. Allerton Conf. Commun., Contr., Comput.*, Oct. 2012, pp. 815–822.
- [49] Y. Ma, J. Zhu, and D. Baron, "Compressed Sensing via Universal Denoising and Approximate Message Passing," *arXiv:1407.1944*, Jul. 2014.
- [50] M. Nassar, P. Schniter, and B. Evans, "A factor graph approach to joint OFDM channel estimation and decoding in impulsive noise environments," *IEEE Trans. Signal Process.*, vol. 62, no. 6, pp. 1576–1589, Mar. 2014.
- [51] M. Nabae and F. Labeau, "Bayesian quantized network coding via generalized approximate message passing," in *Proc. Wireless Telecommun. Symp. (WTS)*, Apr. 2014, pp. 1–7.
- [52] P. Schniter, "A message-passing receiver for BICM-OFDM over unknown clustered-sparse channels," *Proc. Intl. Workshop IEEE Sig. Proc. Adv. Wireless Commun. (SPAWC)*, pp. 246–250, Jun. 2011.
- [53] S. Wu, L. Kuang, Z. Ni, J. Lu, D. Huang, and Q. Guo, "Low-complexity iterative detection for large-scale multiuser MIMO-OFDM systems using approximate message passing," *IEEE J. Sel. Topics Signal Process.*, vol. 8, no. 5, pp. 902–915, Oct. 2014.
- [54] D. Guo and S. Verdú, "Replica analysis of large-system CDMA," *Proc. IEEE Inf. Theory Workshop (ITW)*, pp. 22–25, Mar. 2003.
- [55] M. Mezard and A. Montanari, *Information, Physics, and Computation*. Oxford University Press, Inc., 2009.
- [56] M. Bayati and A. Montanari, "The LASSO risk for Gaussian matrices," *IEEE Trans. Inf. Theory*, vol. 58, no. 4, pp. 1997–2017, Apr. 2012.
- [57] D. Guo, S. Shamai, and S. Verdú, "Mutual information and minimum mean-square error in gaussian channels," *IEEE Trans. Inf. Theory*, vol. 51, no. 4, pp. 1261–1282, Apr. 2005.
- [58] Y. Wu and S. Verdú, "MMSE dimension," *Proc. IEEE Int. Symp. Inf. Theory (ISIT)*, pp. 1463–1467, Jun. 2010.
- [59] C. Jeon, A. Maleki, and C. Studer, "On the performance of mismatched data detection in large MIMO systems," in *Proc. IEEE Int. Symp. Inf. Theory (ISIT)*, Jul. 2016, pp. 180–184.
- [60] S. Verdú, *Multiuser Detection*. Cambridge University Press, 1998.
- [61] J. Jaldén and B. Ottersten, "On the complexity of sphere decoding in digital communications," *IEEE Trans. Signal Process.*, vol. 53, no. 4, pp. 1474–1484, Apr. 2005.
- [62] D. Seethaler, J. Jaldén, C. Studer, and H. Bölcskei, "On the complexity distribution of sphere decoding," *IEEE Trans. Inf. Theory*, vol. 57, no. 9, pp. 5754–5768, Sept. 2011.
- [63] B. Hochwald and S. Ten Brink, "Achieving near-capacity on a multiple-antenna channel," *IEEE Trans. Commun.*, vol. 51, no. 3, pp. 389–399, March 2003.
- [64] C. Studer, A. Burg, and H. Bölcskei, "Soft-output sphere decoding: Algorithms and VLSI implementation," *IEEE J. Sel. Areas Commun.*, vol. 26, no. 2, pp. 290–300, Feb. 2008.

- [65] C. Studer and H. Bölcskei, “Soft-input soft-output single tree-search sphere decoding,” *IEEE Trans. Inf. Theory*, vol. 56, no. 10, pp. 4827–4842, Oct. 2010.
- [66] T. Narasimhan and A. Chockalingam, “Channel hardening-exploiting message passing (CHEMP) receiver in large-scale MIMO systems,” *IEEE J. Sel. Topics Signal Process.*, vol. 8, no. 5, pp. 847–860, Oct. 2014.
- [67] K. Alnajjar, P. Smith, and G. Woodward, “Low complexity V-BLAST for massive MIMO,” in *Proc. Aus. Commun. Theory Workshop (AusCTW)*, Feb. 2014, pp. 22–26.
- [68] M. Čirkić and E. Larsson, “SUMIS: Near-optimal soft-in soft-out MIMO detection with low and fixed complexity,” *IEEE Trans. Signal Process.*, vol. 62, no. 12, pp. 3084–3097, Jun. 2014.
- [69] P. Suthisopapan, K. Kasai, V. Imtawil, and A. Meesomboon, “Approaching capacity of large MIMO systems by non-binary LDPC codes and MMSE detection,” in *Proc. IEEE Int. Symp. Inf. Theory (ISIT)*, Jul. 2012, pp. 1712–1716.
- [70] J. W. Choi, B. Lee, B. Shim, and I. Kang, “Low complexity detection and precoding for massive MIMO systems,” in *Proc. IEEE Wireless Commun. Netw. Conf. (WCNC)*, April 2013, pp. 2857–2861.
- [71] C.-C. Wang and D. Guo, “Belief propagation is asymptotically equivalent to MAP detection for sparse linear systems,” in *Proc. Allerton Conf. Commun., Contr., Comput.*, 2006, pp. 926–935.
- [72] L. Zheng, A. Maleki, X. Wang, and T. Long, “Does  $\ell_p$ -minimization outperform  $\ell_1$ -minimization?” *arXiv:1501.03704*, Jan. 2015.
- [73] G. Reeves and H. D. Pfister, “The replica-symmetric prediction for compressed sensing with Gaussian matrices is exact,” in *Proc. IEEE Int. Symp. Inf. Theory (ISIT)*, Jul. 2016, pp. 665–669.
- [74] D. L. Donoho and J. Tanner, “Counting the faces of randomly-projected hypercubes and orthants, with applications,” *Discrete Comput. Geometry*, vol. 43, no. 3, pp. 522–541, Apr. 2010.
- [75] —, “Precise undersampling theorems,” *Proc. IEEE*, vol. 98, no. 6, pp. 913–924, 2010.
- [76] T. Tanaka, “Analysis of bit error probability of direct-sequence CDMA multiuser demodulators,” in *NIPS*, 2000, pp. 315–321.
- [77] D. Pirjol, “The logistic-normal integral and its generalizations,” *J. Comput. Appl. Math.*, vol. 237, no. 1, pp. 460–469, Jan. 2013.
- [78] G. E. Crooks, “Logistic approximation to the logistic-normal integral,” Lawrence Berkeley National Laboratory, Tech. Rep. 002v4, 2013.
- [79] E. Demidenko, *Generalized Linear Mixed Models*. John Wiley & Sons, Inc., 2005, pp. 329–430.
- [80] A. Kuriya and T. Tanaka, “Performance degradation of AMP for small-sized problems,” in *Proc. IEEE Int. Symp. Inf. Theory (ISIT)*, vol. Jun., 2015, pp. 2802–2806.
- [81] —, “Effects of the approximations from BP to AMP for small-sized problems,” in *Proc. IEEE Int. Symp. Inf. Theory (ISIT)*, Jul. 2016, pp. 770–774.
- [82] S. Rangan, P. Schniter, and A. Fletcher, “On the convergence of approximate message passing with arbitrary matrices,” in *Proc. IEEE Int. Symp. Inf. Theory (ISIT)*, June 2014, pp. 236–240.
- [83] O. Mangasarian and B. Recht, “Probability of unique integer solution to a system of linear equations,” *Eur. J. Oper. Res.*, vol. 214, no. 1, pp. 27–30, Oct. 2011.
- [84] C. Studer, T. Goldstein, W. Yin, and R. G. Baraniuk, “Democratic representations,” *arXiv:1401.3420*, Apr. 2015.
- [85] C. Thrampoulidis, E. Abbasi, W. Xu, and B. Hassibi, “BER analysis of the box relaxation for BPSK signal recovery,” in *Proc. IEEE Int. Conf. Acoust., Speech, Signal Process. (ICASSP)*, Mar. 2016, pp. 3776–3780.
- [86] C. Thrampoulidis, E. Abbasi, and B. Hassibi, “Precise error analysis of regularized  $M$ -estimators in high dimensions,” *IEEE Trans. Inf. Theory*, vol. 64, no. 8, pp. 5592–5628, Aug. 2018.
- [87] C. Thrampoulidis, W. Xu, and B. Hassibi, “Symbol error rate performance of box-relaxation decoders in massive mimo,” *IEEE Trans. Signal Process.*, vol. 66, no. 13, pp. 3377–3392, Jul. 2018.

- [88] C. Rush and R. Venkataramanan, "Finite-sample analysis of approximate message passing," in *Proc. IEEE Int. Symp. Inf. Theory (ISIT)*, Jul. 2016, pp. 755–759.
- [89] Y. Ma, D. Baron, and A. Beirami, "Mismatched estimation in large linear systems," in *Proc. IEEE Int. Symp. Inf. Theory (ISIT)*, Jun. 2015, pp. 760–764.
- [90] D. Guo, Y. Wu, S. Shamaï, and S. Verdú, "Estimation in Gaussian noise: Properties of the minimum mean-square error," *IEEE Trans. Inf. Theory*, vol. 57, no. 4, pp. 2371–2385, Apr. 2011.